Zhang *et al. Microstructures* 2024;4:2024043
DOI: 10.20517/microstructures.2023.93

Microstructures

Review

Open Access

Check for updates

Modulation strategies of electrocatalysts for 5-hydroxymethylfurfural oxidation-assisted water splitting

Tongxue Zhang[1,#], Shuai Liu[1,#], Fumin Wang[1], Wenxian Liu[2], Xinyuan He[1], Qian Liu[3], Xubin Zhang[1], Xijun Liu[4,5]

[1]School of Chemical Engineering and Technology, Tianjin University, Tianjin 300350, China.
[2]College of Materials Science and Engineering, Zhejiang University of Technology, Hangzhou 310014, Zhejiang, China.
[3]Institute for Advanced Study, Chengdu University, Chengdu 610106, Sichuan, China.
[4]State Key Laboratory of Featured Metal Materials and Life-cycle Safety for Composite Structures, MOE Key Laboratory of New Processing Technology for Nonferrous Metals and Materials, School of Resources, Environment and Materials, Guangxi University, Nanning 530004, Guangxi, China.
[5]Guangxi Key Laboratory of Electrochemical Energy Materials, School of Chemistry and Chemical Engineering, Guangxi University, Nanning 530004, Guangxi, China.
[#]Authors contributed equally.

Correspondence to: Assoc. Prof. Wenxian Liu, College of Materials Science and Engineering, Zhejiang University of Technology, Hangzhou 310014, Zhejiang, China. E-mail: liuwx@zjut.edu.cn; Prof. Xubin Zhang, School of Chemical Engineering and Technology, Tianjin University, Tianjin 300350, China. E-mail: tjzxb@tju.edu.cn; Prof. Xijun Liu, State Key Laboratory of Featured Metal Materials and Life-Cycle Safety for Composite Structures, MOE Key Laboratory of New Processing Technology for Nonferrous Metals and Materials, School of Resources, Environment and Materials, Guangxi University, Nanning 530004, Guangxi, China. E-mail: xjliu@gxu.edu.cn

How to cite this article: Zhang T, Liu S, Wang F, Liu W, He X, Liu Q, Zhang X, Liu X. Modulation strategies of electrocatalysts for 5-hydroxymethylfurfural oxidation-assisted water splitting. *Microstructures* 2024;4:2024043. https://dx.doi.org/10.20517/microstructures.2023.93

Received: 22 Dec 2023 **First Decision:** 15 Jan 2024 **Revised:** 27 Jan 2024 **Accepted:** 6 Feb 2024 **Published:** 24 Jul 2024

Academic Editor: Jianfeng Mao **Copy Editor:** Fangyuan Liu **Production Editor:** Fangyuan Liu

Abstract

To address energy shortages and environmental issues, prioritizing renewable energy development and usage is crucial. Employing renewable sources for water electrolysis offers a sustainable method for hydrogen generation. Reducing the water electrolysis potential is vital for efficient clean energy conversion and storage. Substituting the anodic oxygen evolution reaction in conventional hydrogen production from water electrolysis with the more thermodynamically favorable 5-hydroxymethylfurfural (HMF) oxidation reaction can greatly decrease overpotential and yield the valuable product 2,5-furan dicarboxylic acid. The key to this process is developing effective electrocatalysts to minimize the potential of the HMF electrooxidation-hydrogen production system.

Therefore, this review provides a comprehensive introduction to the modulation strategies that affect the electronic and geometric structure of electrocatalysts for HMF oxidation-assisted water splitting. The strategies encompass heteroatom doping, defect projection, interface engineering, structural design, and multi-metal synergies. The catalysts are assessed from various angles, encompassing structural characterization, reaction mechanisms, and electrochemical performance. Finally, current challenges in the catalyst design and potential development of this promising field are proposed.

Keywords: 5-hydroxymethylfurfural, hydrogen evolution reaction, control strategy, electronic structure, electrocatalysis

INTRODUCTION

The rapid progression of the global economy and society has led to a marked increase in energy demand. Nonetheless, the finite fossil fuels available on Earth, such as coal and oil, are swiftly depleted. Additionally, their ongoing emissions of harmful gases such as CO_2 and SO_2 contribute to various environmental issues, posing significant threats to human health and food security[1-7]. This situation necessitates a focus on developing a safe and sustainable system for energy use. To address the pressing concerns of energy scarcity and environmental deterioration, people are actively exploring alternative renewable energy sources, such as wind and solar energy, as substitutes for fossil fuels. Nonetheless, the intermittent and unpredictable nature of these sources poses a hindrance to their consistent utilization[8-10]. Therefore, the urgency lies in the need for advancing renewable energy storage and conversion technologies[11,12]. Hydrogen energy has garnered significant interest for its diverse sources and applications, high energy density and calorific value[13,14]. Consequently, it is poised to serve as a pivotal green energy carrier in the sustainable energy sector. Utilizing renewable energy-driven water electrolysis for hydrogen production is a promising energy strategy[15-17], especially when compared to conventional methods such as coal gasification and methane steam reforming which emit carbon. Water electrolysis offers advantages such as simple equipment and stable processes, making it economical and scalable for hydrogen production. Consequently, this method has emerged as a pivotal energy conversion and storage technology.

The electrochemical water electrolysis consists of two reactions: the hydrogen evolution reaction (HER) and the oxygen evolution reaction (OER)[18]. Figure 1 illustrates that when an external potential is applied, electrons reach the cathode through the external circuit; hydrogen protons receive electrons at the cathode to generate hydrogen gas, and hydroxide ions lose electrons at the anode to generate oxygen. The specific chemical reaction equations in the electrolytic cell vary slightly depending on the pH of the electrolyte[19]. Although acidic conditions facilitate the HER process and alkaline conditions facilitate the OER process, hydrogen production in industrial settings is mainly carried out under alkaline conditions. This is due to the susceptibility of acidic conditions to equipment corrosion, resulting in low economic benefits[20]. Furthermore, the overall efficiency of water decomposition is significantly influenced by the rate of the OER reaction, as the OER is more kinetically sluggish than the HER at the cathode.

According to data from the International Energy Agency, it is projected that the market share of hydrogen production from electrolysis of water will reach approximately 22% by 2050. Although over two centuries have passed since Deiman discovered water electrolysis in 1789[21], the majority of hydrogen gas is currently generated through coal gasification and fossil fuel reforming. The contribution of hydrogen produced by electrolytic water is less than 4% of the global hydrogen production[22,23], indicating significant potential for improvement in practical applications. The main factors limiting the widespread application of water electrolysis for hydrogen production include the following aspects:

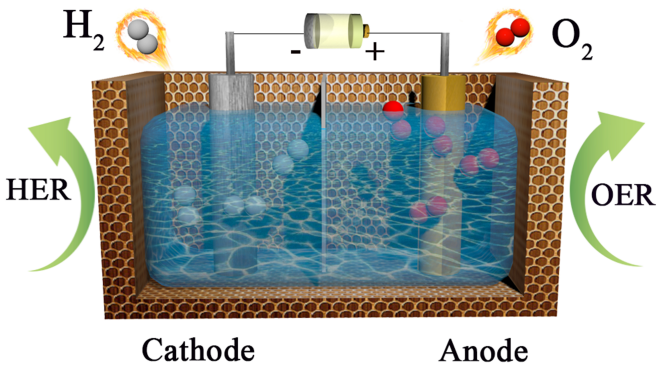

Figure 1. Diagram of water splitting device.

(1) The thermodynamic potential of OER is high as 1.23 V;

(2) OER involves the four electrons coupled protons transfer process, and its kinetic reaction rate is slow;

(3) The amount of oxygen produced through natural photosynthesis is sufficient to fulfill the demands of the global chemical industry, and the added value of anodic reaction is relatively low;

(4) To prevent the explosion of H_2 and O_2 gas mixtures generated during the electrolysis process, a separate compartment must be designed, which results in high costs[24,25]. Moreover, even proton exchange membranes (PEM) still cannot completely avoid the explosive formation.

These limitations significantly hinder the overall efficiency of energy conversion and the potential applications of water decomposition. In recent years, researchers have shifted their focus to a novel hybrid water electrolysis method that combines HER with electrooxidation reactions of organic small molecules. Currently, the anodic OER is primarily substituted by thermodynamically more favorable oxidation of organic molecules such as urea[26], hydrazine[27], alcohol[28,29], and (5-hydroxymethyl) furfural[30]. The bond dissociation energy of the "C-H" and "O-H" bonds in these organic substrates is considerably lower than that of the "O-H" bond in water[31], which can reduce the water decomposition potential and produce high value-added products or degrade pollutants at the anode. It is an effective way to reduce consumption and enhance economic value[32].

Among the numerous replaceable organic molecules, biomass, as the most abundant carbon-containing renewable resource on Earth, offers several advantages such as affordability, minimal pollution, and broad application scope. Biomass predominantly forms through the natural conversion of CO_2 and H_2O into carbohydrates via photosynthesis[33-35]. By utilizing efficient conversion methods, non-grain carbon resources can be transformed into high-value chemicals, meeting the growing demand of the chemical industry and addressing environmental pollution and energy shortages. 5-Hydroxymethylfurfural (HMF) is derived from biomass through acid-catalyzed dehydration of C6 carbohydrates. It is affordable and widely found in various sugar-containing natural substances such as honey, milk, and raisins. Additionally, HMF is a compound formed by the Maillard reaction in most carbohydrates. This compound is considered the most important among the numerous platform compounds obtained from biomass energy conversion and

is widely regarded as a crucial link between biomass energy and the fossil energy industry, as well as other fine chemical industries. It possesses a furan ring, hydroxyl (OH), and aldehyde group (C=O)[36]. Due to its unique chemical structure, HMF enables various reactions such as oxidation, hydrogenation, condensation, hydrolysis, and halogenation, thereby producing a series of chemically valuable fine products. Among them, the economic value of its oxidation product 2,5-furan dicarboxylic acid (FDCA) is particularly outstanding. Following two oxidation processes, HMF can be further upgraded to FDCA. The electrode reaction and total reaction equation are as follows:

$$\text{Anode: HMF} + 6OH^- \rightarrow \text{FDCA} + 4H_2O + 6e^- \quad (1)$$

$$\text{Cathode: } 6H_2O + 6e^- \rightarrow 3H_2 + 6OH^- \quad (2)$$

$$\text{Overall: HMF} + 2H_2O \rightarrow \text{FDCA} + 3H_2 \quad (3)$$

There are two conversion paths from HMF to FDCA [Figure 2]:

The hydroxyl group of HMF in route 1 is first oxidized to DFF (2,5-diformylfuran), and the aldehyde group of HMF in route 2 is initially oxidized to HMFCA (5-hydroxymethyl-2-furancarboxylic acid). Both DFF and HMFCA will be upgraded to FFCA (5-formyl-2-furancarboxylic acid) and then converted to FDCA[37]. FDCA is a highly promising chemical regarded as one of the most promising chemicals among the 12 biomass-derived value-added chemicals announced by the US Department of Energy in 2004[38,39]. It has a melting point of 342 °C, good stability, and insolubility in common organic and inorganic solvents[40-42]. As a key compound in the field of bio-based platform chemicals, FDCA finds extensive applications in various industries, including pharmaceuticals, dyes, and molecular recognition[43,44]. In addition, FDCA can be polymerized to form polyglycol furan diformate (PEF). PEF is easier to degrade compared to traditional petroleum-derived polyethylene terephthalate (PET). PEF also shows significant improvements in key properties such as CO_2 barrier, O_2 barrier, and tensile strength. Therefore, FDCA, as a substitute for traditional petroleum-derived products, has strong prospects for development. According to statistics from the US Department of Energy, there is a market demand of at least nine billion annually for FDCA-derived products, which is much larger than the four billion market size for PET. In conclusion, the controlled and efficient conversion of HMF into FDCA has significant commercial value.

HMF electrooxidation reaction (HMFOR) offers several advantages over traditional HMF oxidation methods. It operates under mild reaction conditions at room temperature and atmospheric pressure, eliminating the need for additional additives or oxidants[45-49]. Moreover, it yields a high FDCA output. Another benefit is that the standard electrooxidation potential of HMF (0.30 V) is significantly lower than that of OER (1.23 V)[48,50], making HMF electrochemical selective oxidative coupling for hydrogen production an efficient means of improving energy utilization efficiency[51]. Overall, this sustainable strategy promises both effectiveness and economic benefits for production.

Despite the early report by Grabowski *et al.*[52] in 1991 on the electrochemical oxidation of HMF to FDCA, significant advancements in HMFOR research have only emerged recently. Although HMFOR coupled with HER for FDCA and H_2 production can achieve a combined theoretical Faraday efficiency (FE) of nearly 200%[53-56], malignant competition of OER is inevitable in aqueous solutions[45]. Despite its ability to accelerate the electrochemical oxidation reaction of HMF under high pH conditions, Vuyyuru *et al.* observed that HMF is prone to degradation into humic products in highly alkaline solutions, which is not conducive to the occurrence of the reaction[57]. To mitigate excessive degradation of HMF, it is crucial to

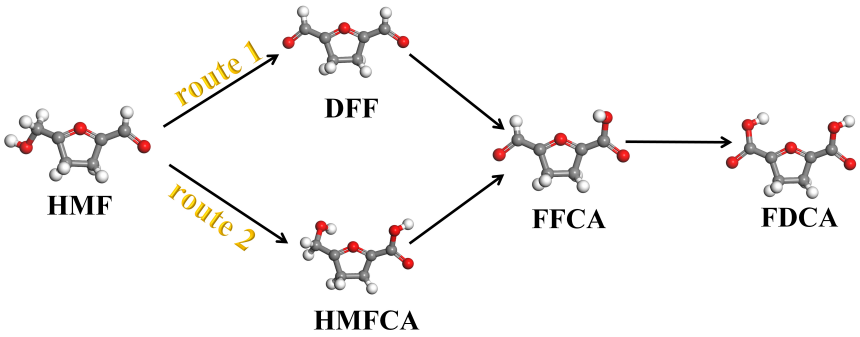

Figure 2. Schematic diagram of HMF oxidation.

enhance the activity of HMFOR through improved electrocatalysts, thereby reducing the electrolysis time. Cha *et al.* utilized costly electrodes, Au and Pt, to facilitate the oxidation of HMF in a redox medium (2,2,6,6-tetramethylpiperidine 1-oxyl, TEMPO), resulting in high FDCA yield and FE[58]. However, the high cost associated with these electrodes is undesirable. Therefore, the development of efficient non-precious metal catalysts for this electrochemical coupling system is imperative in addressing the comprehensive cost and benefit concerns.

Extensive research has been conducted on the use of non-precious metal-based electrocatalysts, such as oxide, hydroxide, nitride, phosphide, and sulfide, to reduce the initial potential of HMFOR[59-65]. Barwe *et al.* used nickel foam (NF) modified by nickel boride (Ni_xB) with high surface area as an electrode for HMFOR and achieved FE close to 1[65]. You *et al.* reported the use of a Ni_2P nanoparticle array (Ni_2P NPA/NF) grown on NF as a bifunctional electrocatalyst for HMF oxidation and hydrogen evolution in an alkaline medium[66]. In an electrolytic cell using Ni_2P NPA/NF as a dual electrode, the potential required at the same current density was at least 200 mV lower compared to pure water splitting. Despite the promising activity exhibited by these transition metal compounds, their high intrinsic redox potential or slow kinetics limit their performance in meeting the actual requirements of hydrogen production[67]. The performance of HMFOR-assisted hydrogen production systems still needs to be optimized. Research has indicated that modifying the geometric features and electronic structure of catalysts can enhance their conductivity, increase the number of effective active sites, optimize the adsorption of intermediates and desorption of products, and further improve the electrocatalytic performance of materials. Various modulation strategies can be employed to achieve alterations in the geometric characteristics and electronic structure of catalysts for HMF oxidation-assisted water splitting systems toward high-value-added chemical production and energy-efficient H_2 generation. Considering the rapid development of this field, a timely systematic review paper is urgently needed.

However, the reported reviews of HMF electrooxidation mainly focused on alloy catalyst regulation, various types of catalysts, and reaction pathways and mechanisms[45,68,69]; there is currently a lack of comprehensive and in-depth summary on the latest design and synthesis strategies of electrocatalyst in HMF oxidation-assisted water splitting. It is crucial to timely review the progress in this research field in order to significantly inspire future studies. In this review, we systematically categorize strategies the modulation strategies that affect the HMF electrooxidation-coupled hydrogen production system through heteroatom doping, defect projection, interface engineering, structural design, and multi-metal synergies. Subsequently, the progress in various regulatory approaches within the HMFOR and HER coupled systems was discussed, evaluating catalyst performance using metrics such as overpotential, HMF conversion rate, FDCA yield, and FE. Finally, the optimization strategy of HMFOR-assisted hydrogen production systems is prospected.

CATALYST MODULATION STRATEGIES

Heteroatom doping

Heteroatom doping is recognized as an effective approach to enhance the intrinsic activity of catalysts while keeping the crystal phase of the original material unchanged, with only slight modifications in the lattice. By introducing doping agents, the charge distribution and coordination environment of the catalyst can be altered, leading to an improvement in the electronic structure of the material. This increases the number of active sites and optimizes the adsorption of intermediates and desorption of products[70-74]. Doping can be categorized into cation doping, anion doping, and cation/anion co-doping, depending on the type of dopant used. Currently, cation doping is the predominant method employed in reported HMFOR-OER systems, while transition metals with empty d orbitals are often used as cation dopants. For instance, doping metal elements, such as Fe, Co, and Cu, close to Ni into Ni-based compounds proves to be an effective strategy as it enhances the electrochemically active surface area and facilitates electron transfer[75-77].

Sun *et al.* conducted a study in which they synthesized Co-doped Ni_3S_2 (expressed as Co_xNiS@NF) and utilized it as an electrocatalyst for HMFOR under alkaline conditions[70]. X-ray diffractometer (XRD) analysis reveals that the introduction of Co doping led to lattice distortion and reduced crystallinity of Ni_3S_2 [Figure 3A and B], resulting in Co_xNiS@NF possessing a higher number of active sites. X-ray photoelectron spectroscopy (XPS) analysis demonstrates that compared to undoped Ni_3S_2, $Co_{0.4}NiS$@NF exhibited a 0.4 eV increase in the binding energy of the Ni 2p peak [Figure 3C], indicating that Co doping may influence the electronic structure of the Ni center. Furthermore, *in situ* Raman studies in Figure 3D-F indicate that $Co_{0.4}NiS$@NF is rapidly reconstructed as NiCo (oxy)hydroxide, which reduces the potential threshold and serves as the actual active site for OER and HMFOR. The optimized $Co_{0.4}NiS$@NF catalyst displays an exceptionally low starting potential (0.9 V *vs.* RHE) and a high current density (497 mA cm^{-2}) at 1.45 V [Figure 3G]. The electrooxidation kinetics show that Co doping reduced the Tafel slope and the charge transfer resistance [Figure 3H and I], indicating enhanced electron transfer rates achievable through Co doping.

Cai *et al.* successfully synthesized nanosheets of 2D metal-organic frameworks (MOFs) through the coordination of Ni^{2+} ions and terephthalic acid (BDC) ligands and further improved the FE oxidation of HMF by stabilizing high valent nickel ions with metal doping (Co, Fe, Mn)[78]. The resulting NiBDC nanosheets can be observed in Figure 4 to grow uniformly and vertically on NF, exposing a large number of surface active sites and pores. The introduction of metal doping does not significantly alter the initial 2D nanosheets morphology of NiBDC, and the doped metals can be uniformly dispersed along with Ni and O. Research has shown that the appropriate doping of metals and ligands can promote the formation of high valent Ni species. Among the doped samples, Co-doped NiCoBDC NF exhibits the highest activity for HMF electrooxidation. Thanks to the presence of abundant exposed active sites and the synergistic effect between Ni and Co atoms, the 2D NiCoMOFs demonstrate both high catalytic activity and excellent electrochemical durability.

In addition to Ni-based compounds, doping heteroatoms in other transition metal catalysts has also been proven to be an effective method for regulating electronic structure and improving their intrinsic activity for HMFOR and/or HER. For instance, Xie *et al.* developed and optimized a Ce-doped Co_2P nanoparticle array anchored in nitrogen carbon nanoarrays using a straightforward MOF template strategy (represented as Ce-Co_2P@NC)[79]. This array served as a dual-functional electrocatalyst for HMFOR coupled with HER systems. The addition of Ce allows for the optimization of the electronic structure of Co-based catalysts and substantially improves their electrocatalytic activity. Theoretical calculations further indicate that Ce doping facilitates electron transfer between the active phase and the reaction substrate HMF and decreases the free

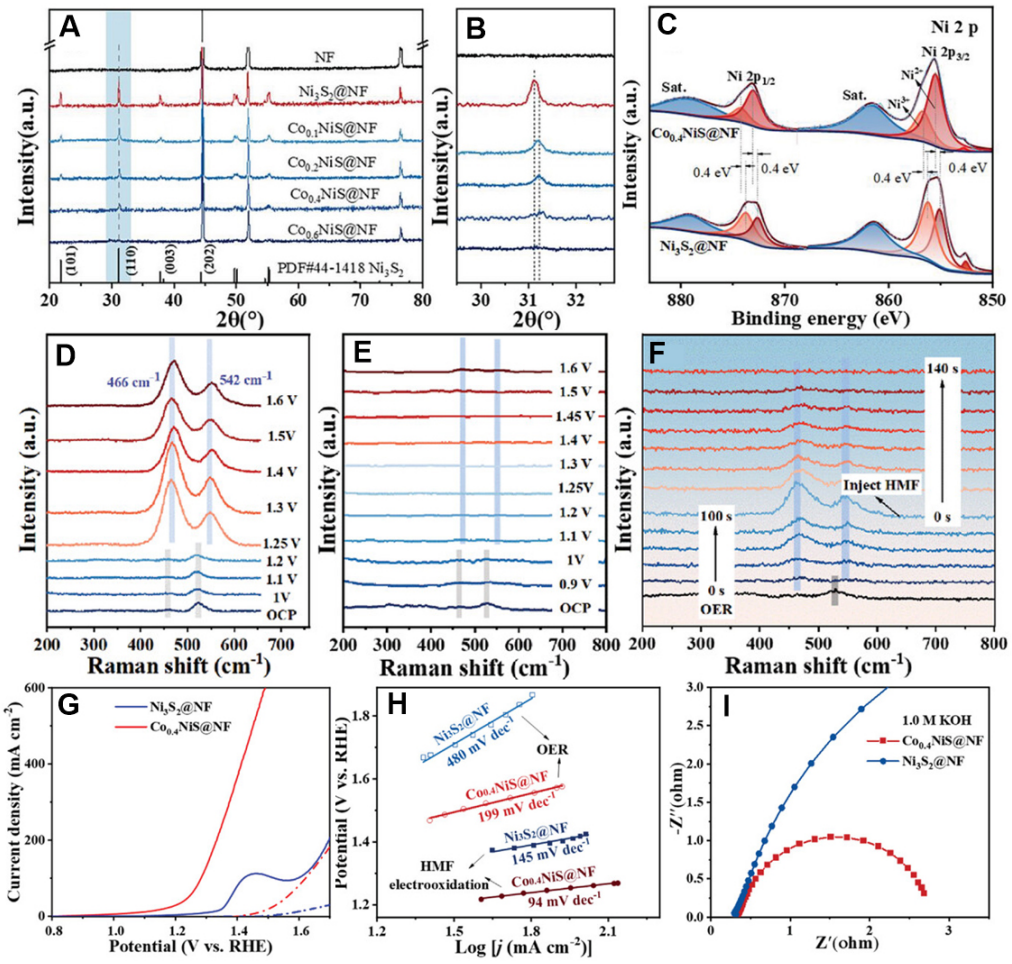

Figure 3. (A) XRD of the as-synthesized Ni_3S_2@NF, Co_xNiS@NF, and NF. (B) Corresponding enlarged XRD patterns. (C) XPS spectra of Ni 2p for $Co_{0.4}NiS$@NF and Ni_3S_2@NF. *In situ* Raman spectra of $Co_{0.4}NiS$@NF electrodes during (D) OER (1.0 M KOH) and (E) HMFOR (1.0 M KOH with 50 × 10^{-3} M HMF) under increasing potential from OCP to 1.6 V. (F) *In situ* Raman spectra of $Co_{0.4}NiS$@NF electrodes during OER (1.0 M KOH) and half-way injected HMF (10 × 10^{-3} M HMF) under 1.45 V. (G) Linear sweep voltammetry (LSV) curve. (H) Tafel plots. (I) Nyquist. Reproduced with permission[70]. Copyright 2022, Wiley.

energy barrier for dehydrogenation of the intermediate (*HMFCA) (from Co_2P@NC 0.58 eV to Ce-Co_2P@NC 0.36 eV), demonstrating the important role of Ce doping in this process.

Li *et al.* used electrodeposition and phosphating strategies to prepare nickel-doped Co_2P (Ni-Co_2P) nanoflake catalysts using Ni species released *in situ* from defective NF as a metal source [Figure 5A][80]. The initial precursor Ni-$Co(OH)_2$ consists of smooth and interconnected nanosheets measuring several hundred nanometers. The surface of the product becomes rough and curly after being transformed into Ni-Co_3O_4. The phosphating treatment does not significantly alter the structure, but it creates numerous voids on the surface of nanosheets [Figure 5B-D], resulting in a larger surface area and improving mass transfer for electrochemical reactions. The high-angle annular dark-field scanning transmission electron microscopy (HAADF-STEM) image reveals a lattice spacing of 2.21 Å, corresponding to the (111) plane of Co_2P [Figure 5E], indirectly confirming the presence of doped Ni as a single atom. Density functional theory (DFT) calculations indicate that the doping of Ni can improve the adsorption of reactants and reduce the reaction energy barrier [Figure 5F and G]. The optimized Ni-Co_2P catalyst exhibits remarkable electrocatalytic activity and stability in HMFOR at an ultra-low potential of 1.29 V, with FDCA yield (99%) and FE (97%) [Figure 5H and I].

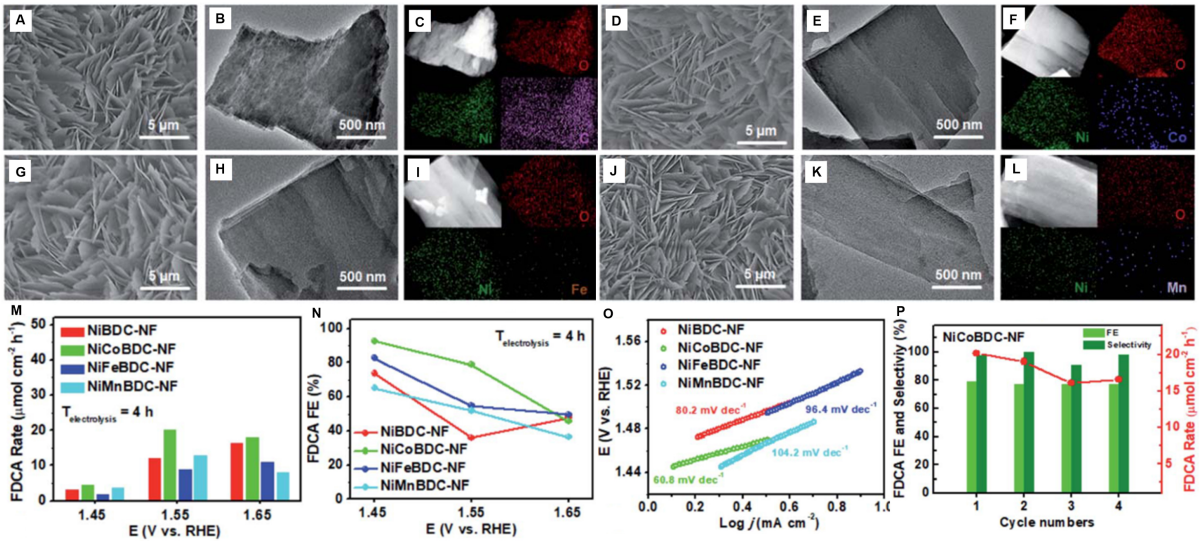

Figure 4. Scanning electron microscope (SEM), transmission electron microscope (TEM), and elemental mapping images of (A-C) NiBDC-NF, (D-F) NiCoBDC-NF, (G-I) NiFeBDC-NF and (J-L) NiMnBDC-NF. (M and N) FDCA yield rate and FE of NiBDC, NiCoBDC, NiFeBDC, and NiMnBDC for 4 h electrolysis. (O) Tafel plots in the presence of HMF. (P) FE, selectivity, and yield rate of FDCA using NiCoBDC-NF during four successive electrolysis. Reproduced with permission[78]. Copyright 2020, Royal Society of Chemistry.

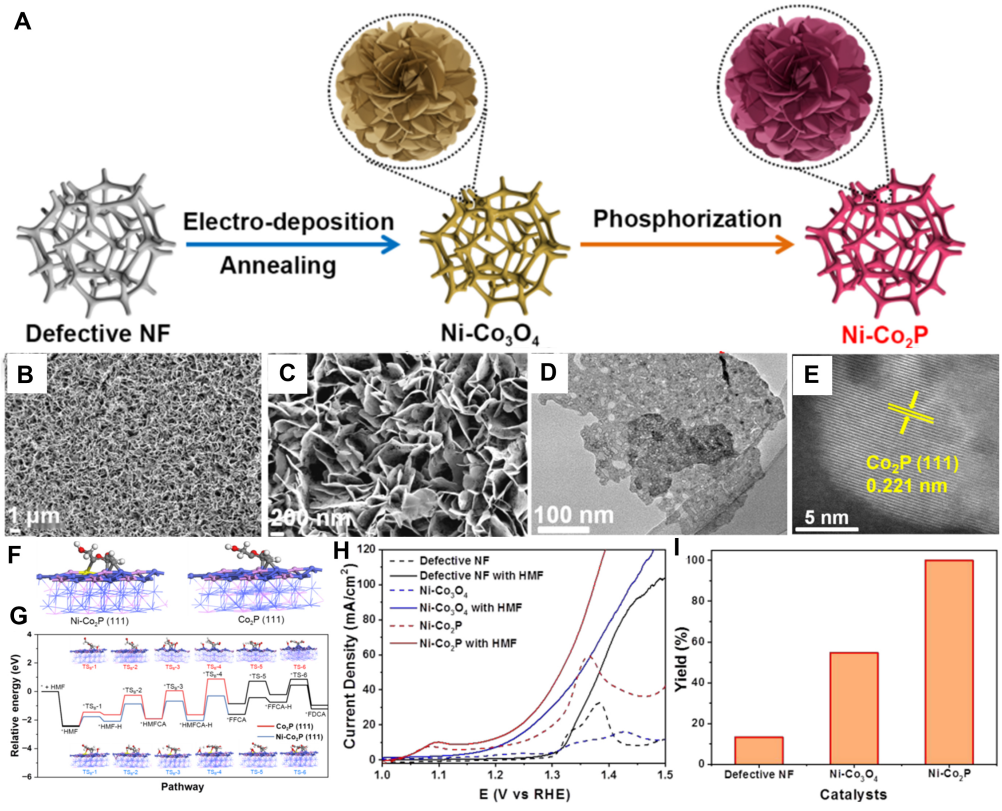

Figure 5. (A) Schematic illustration for the synthesis of Ni-Co_2P catalyst. (B) Low and (C) high magnification SEM images. (D) TEM image. (E) aberration-corrected HAADF-STEM images of Ni-Co_2P catalyst. (F) The optimized geometries for the HMF adsorption structures and (G) energy profiles for the conversion of HMF to FDCA via HMFCA pathway on Ni-Co_2P (111) and Co_2P (111), respectively. (H) LSV curves. (I) FDCA yields for defective NF, Ni-Co_3O_4 and Ni-Co_2P catalyzed HMFOR at 1.29 V (*vs.* RHE). Reproduced with permission[80]. Copyright 2022, Springer Nature.

Defect projection

Defect engineering serves as a highly effective approach for modulating the electronic structure of materials. Introducing defects in the lattice structure can achieve the adjustment of the electronic structure of catalysts at the atomic level. The generation of defects frequently results in alterations in the coordination environment surrounding metal atomic sites, thereby optimizing the binding energy with reaction intermediates, facilitating charge transfer of materials, and subsequently enhancing electrochemical capabilities[81]. The techniques employed for introducing defects mainly encompass alkali etching, element doping, chemical reduction and laser treatment[82-87]. Surface electronic structure adjustment through defect engineering primarily revolves around the introduction of anion and cation vacancies.

Oxygen vacancies have gained significant attention as the most extensively examined anion vacancies in transition metal oxides. The incorporation of oxygen vacancies has been experimentally demonstrated as a successful approach for enhancing electrochemical performance, achieved by altering electrochemically active surfaces and the coordination environment of metal sites[88,89]. Huang *et al.* introduced abundant oxygen vacancies on the surface of CoO by introducing Se[50]. The resulting optimized CoO/$CoSe_2$ (23:1) catalyst demonstrates significantly enhanced catalytic activity for the electrooxidation of HMF to FDCA compared to the original CoO and $CoSe_2$. Specifically, at a potential of 1.43 V *vs.* RHE, the FDCA yield could reach 99%, and the FE is 97.9%. This research indicates that introducing abundant oxygen vacancies on CoO can enhance the activity and selectivity of the catalyst for electrocatalytic oxidation of HMF to FDCA by increasing the electrochemical surface area and reducing the charge transfer resistance. In a separate study, Wang *et al.* prepared NiO catalysts with varying oxygen vacancy contents (V_o-NiO) using a laser ablation strategy for HMFOR, as shown in Figure 6A[90]. The surface adsorption infrared spectrum shows that V_o-NiO exhibits strong adsorption capabilities for C=O and C-OH [Figure 6B], which facilitates the adsorption of HMF. By combining theoretical calculations with *in situ* Raman spectroscopy [Figure 6C-E], the authors proposed a possible mechanism under alkaline conditions: the oxygen vacancies in the catalyst can be first filled by ·OH in the solution, promoting the pre-oxidation of low valent Ni at low oxidation potential, which was beneficial for catalyst surface reconstruction. Additionally, the oxygen vacancies increased the density of states near the Fermi level of V_o-NiO and enhanced the electron conduction rate. Therefore, V_o-NiO demonstrates the most superior performance in terms of HMFOR [Figure 6F].

Zhang *et al.* conducted a two-step process involving the hydrothermal method and electrochemical cycle voltammetry to create ultra-thin wrinkled NiVW LMH (LMH is an ultra-thin two-dimensional metal hydroxide) with abundant lattice vacancies. Compared with the original $Ni(OH)_2$, the NiV LMH introduced with a small amount of vanadium maintains the same crystal structure and phase while exhibiting a relatively flat nanosheet structure [Figure 7A and B][91]. The addition of tungsten induces lattice distortion and gives the catalyst a unique folded structure. During the subsequent electrochemical treatment process, the morphology of the nanosheets does not change [Figure 7C and D]. The dissolution of vanadium and tungsten atoms facilitates the formation of lattice vacancies [Figure 7E and F], altering the local coordination environment of Ni cations and exposing more unsaturated Ni active sites, thereby enhancing the production of Ni(OH)O reaction species. Atomic force microscopy (AFM) confirms the ultra-thin structure of the nanosheets, measuring 1.6 nm in height [Figure 7G and H]. This thin structure reduces the diffusion energy of H^+ from Ni^{2+}-OH, leading to an increased dehydrogenation rate and improving the oxidation activity of HMF. The current density of HMFOR on NiVW LMH with abundant lattice vacancies electrocatalyst can reach 193 mA cm^{-2} at 1.43 V *vs.* RHE, which is 5.37 times higher than that of $Ni(OH)_2$ electrode [Figure 7I]. Additionally, Figure 7J displays a high conversion rate of HMF (close to 100%) and a high selectivity of FDCA (> 99%).

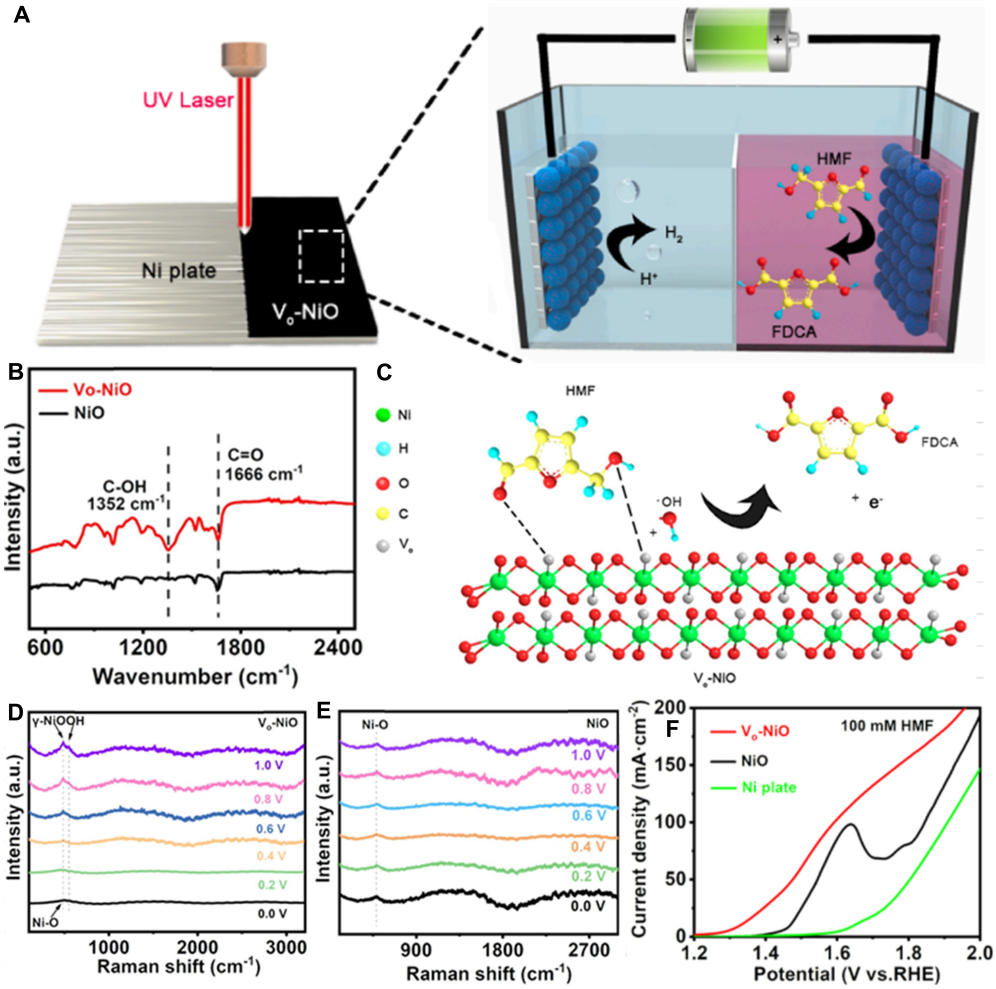

Figure 6. (A) Schematic diagram of synthesis and catalysis of V_o-NiO. (B) Adsorption infrared spectra of HMF on V_o-NiO and NiO surface. (C) The mechanism of HMFOR. *In situ* Raman spectra of prepared (D) V_o-NiO and (E) NiO in 1.0 M KOH with 100 mM HMF at different applied potentials. (F) Polarization curves of V_o-NiO, NiO, and Ni. Reproduced with permission[90]. Copyright 2022, Elsevier.

Furthermore, apart from anion vacancies, the augmentation of catalyst activity for HMF to FDCA conversion has been demonstrated through the presence of metal vacancies (cation vacancies). Qi *et al.* conducted a hydrothermal method and alkaline etching treatment to fabricate carbon paper loaded with nickel-iron layered double hydroxides (LDH) that possessed cation-rich defects (d-NiFe-LDH/CP)[92]. The successful introduction of cationic vacancies is confirmed by electron paramagnetic resonance spectroscopy, and XPS testing indicates that the effective introduction of cationic vacancies could enhance the electronic density of NiFe-LDH and adjust the electronic structure of metal sites. Consequently, this resulted in a significant increase in the number of active sites and a decrease in charge transfer resistance, thus leading to the exceptional catalytic performance of d-NiFe-LDH/CP. At 1.48 V *vs.* RHE, it has an almost complete conversion rate of HMF (97.35%) and a yield of FDCA (96.8%), with an FE of 84.47%. In addition, the catalyst displays outstanding stability over ten cycles.

Interface engineering

Extensive research has been conducted on the interface effect between the carrier and the active catalyst. This effect plays a crucial role in controlling electron distribution and regulating intermediate

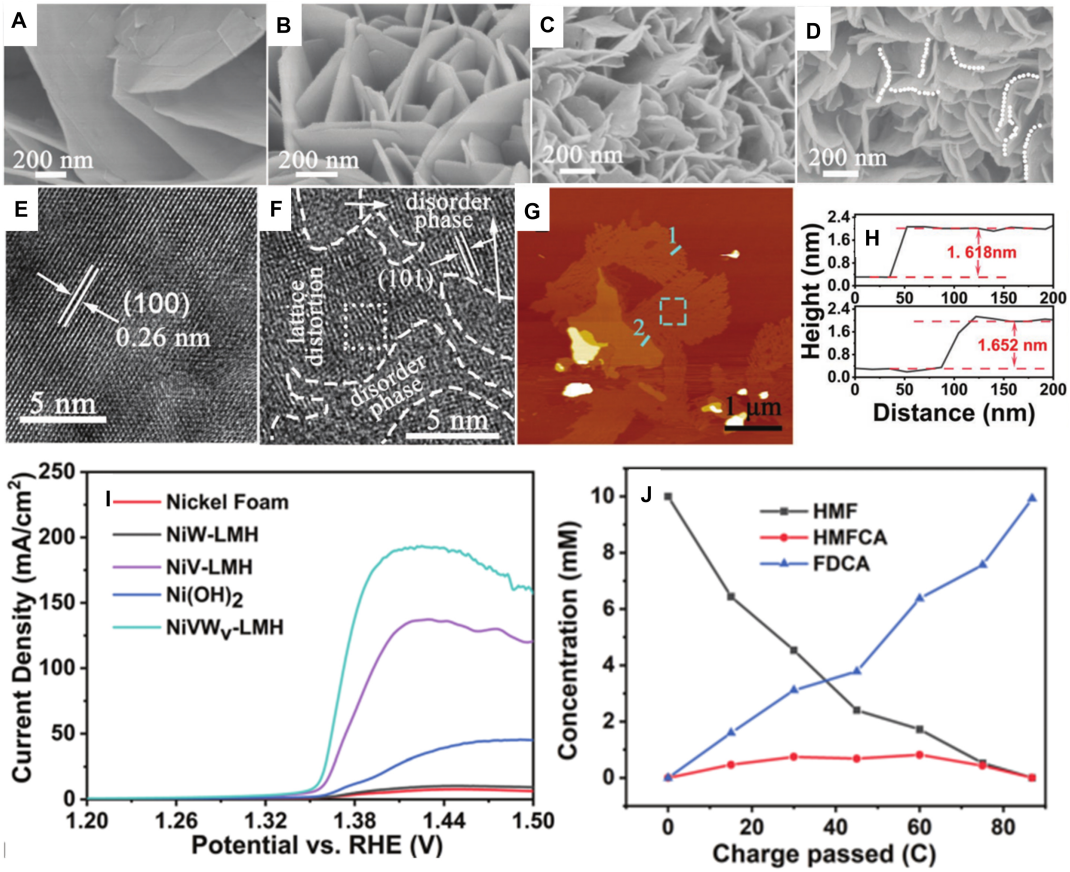

Figure 7. (A) SEM images of $Ni(OH)_2$, (B) NiV-LMH, (C) NiVW-LMH and (D) NiVW-LMH with abundant lattice vacancies. HRTEM images of (E) $Ni(OH)_2$ and (F) NiVW-LMH with abundant lattice vacancies. (G) AFM images and (H) height profiles of NiVW-LMH with abundant lattice vacancies nanosheets. (I) LSV curves with 90% iR correction in 1.0 M KOH solution with 10 mM HMF. (J) The concentration of HMF and its oxidation products during chronoamperometry electrolysis experiment on NiVW-LMH electrode with abundant lattice vacancies. Reproduced with permission[91]. Copyright 2019, Wiley.

adsorption[93-95]. Constructing the metal carrier interface in a well-thought-out manner is highly important for enhancing the intrinsic activity and stability of the catalyst during HMF oxidation.

Zhang *et al.* successfully synthesized Ni_3N/carbon nanosheets (Ni_3N@C) using hydrothermal and nitriding processes[63]. Ni_3N particles adhere to the carbon film to form a sheet-like structure. The carbon film acts as a supportive material, preventing the accumulation of Ni_3N nanoparticles and maintaining the structure of the precursor. The strong interface effect leads to changes in the electronic structure of Ni^+ and enhances the charge transfer rate. Ni_3N@C demonstrates remarkable electrocatalytic performance for both HMFOR and HER. At a current density of 50 mA cm^{-2}, the potential for HMFOR is 1.38 V *vs.* RHE. Pang *et al.* introduced an electrochemical reconstruction strategy to activate the interface of Ni-MOF/Ag[96]. This strategy forms a double-site active interface consisting of Ni^{3+} and Ag^+ species. A series of characterization tests confirm the successful generation of high-valence active species and the stable anchoring of Ag species on the catalyst surface through the formation of NiOOH. The electrochemical treatment induces a change in the morphology of Ag nanoparticles on the Ni film. The activated Ni-MOF/Ag catalyst exhibits exceptional electrocatalytic performance for HMF oxidation, achieving nearly 100% HMF conversion and 98.6% FE at 1.623 V *vs.* RHE.

Furthermore, the implementation of heterogeneous interfaces featuring dual active components is a highly efficient approach in the field of interface engineering. Unlike using a single component, the interface formed by different active components allows for the creation of robust built-in fields through bonding or electronic interactions[97-102]. By designing a heterogeneous structure where two components mutually enhance each other, novel active sites can be generated at the interface, promote electron transfer, and accelerate HMFOR and HER kinetics. Xie *et al.* created a composite catalyst consisting of cobalt hydroxide and cerium dioxide $Co(OH)_2$-CeO_2 through electrodeposition[103]. This catalyst was used for the selective electrocatalytic conversion of HMF under neutral conditions. The induction of CeO_2 greatly promotes the transformation of the main element Co into high-valent active substances, increasing HMFCA products. Under neutral conditions of pH = 7, a mild conversion of HMF to HMFCA is achieved at 1.4 V *vs.* RHE through double electron oxidation of aldehyde groups, with a selectivity of 89.4% and a yield of 85.8%, demonstrating its potential in clean energy.

Wang *et al.* constructed a porous CoP-CoOOH heterojunction electrocatalyst for enhancing HMFOR by adjusting the electron density between interfaces[104]. The synthesis scheme is shown in Figure 8A, where CoOOH is in close contact with CoP to form nanosheets on the nanoneedle structure. Such a three-dimensional network structure can increase the probability of contact with reactants. Theoretical calculations presented in Figure 8B and C reveal that CoP-CoOOH exhibits the highest density of states near the Fermi level, suggesting a greater number of effective electron transfers. Additionally, the adsorption energy calculation of HMF on various catalyst samples demonstrates that CoP-CoOOH enhances the kinetics of HMFOR. XPS tests depicted in Figure 8D-F indicate that electron transfer occurring on the heterojunction surface leads to the accumulation of electrons on CoP, while holes accumulate on CoOOH. This hole accumulation on CoOOH promotes HMF adsorption, while electron transfer to the CoP surface favors the occurrence of HER; the electrochemical performance tests are shown in Figure 8G and H. Furthermore, when combined with a continuous flow reactor, diffusion and reaction rates are accelerated, resulting in improved HMFOR efficiency [Figure 8I].

Guo *et al.* successfully constructed an heterogeneous interface (Cu-Co_3O_4/CuO) between Cu-doped Co_3O_4 and CuO[105]. The presence of mismatched lattice fringes between Co_3O_4 and CuO, along with a clearly defined interface between Cu-Co_3O_4 and CuO in the element mapping image, confirms the formation of the Cu-Co_3O_4/CuO heterogeneous interface [Figure 9A-F]. XPS tests depicted in Figure 9G and H reveal that the peak binding energy of Cu $2p_{3/2}$ in Cu-Co_3O_4/CuO is lower compared to pure CuO, indicating a decrease in Cu valence state and an increase in the Co^{3+}/Co^{2+} ratio (from 1.20 to 1.51), indicating that Co atoms can provide electrons to Cu atoms and there is a strong electronic interaction. Electrochemical studies demonstrate that Cu-Co_3O_4/CuO exhibits higher catalytic activity for the HMFOR reaction compared to Cu-Co_3O_4 and pure Co_3O_4 [Figure 9I]. Meanwhile, the catalytic activity of Cu-Co_3O_4/CuO is superior to that of a product obtained by physically mixing Cu-Co_3O_4 and CuO, highlighting the unique contribution of heterogeneous interfaces to the electrocatalytic ability. Theoretical calculations also indicate that the formation of heterogeneous interfaces enhances the interaction between the electrocatalyst and aldehydes and hydroxymethyl groups, thereby improving the adsorption of HMF by active sites [Figure 9J].

Structural design

Conducting additional research into the structure, distribution of active sites, and kinetics has the potential to facilitate the development of more efficient catalysts in the future. By implementing a reasonable structural design, it becomes possible to increase the exposure of active sites on the catalyst, thereby enhancing surface adsorption and mass transfer capabilities[106,107]. For example, Zhao *et al.* conducted a study on the impact of graded NiCo-S catalysts on the electrooxidation of HMF[108]. SEM images reveal that the surface of NiCo-S nanosheets exhibits a graded and fluffy structure with edge curls [Figure 10A and B].

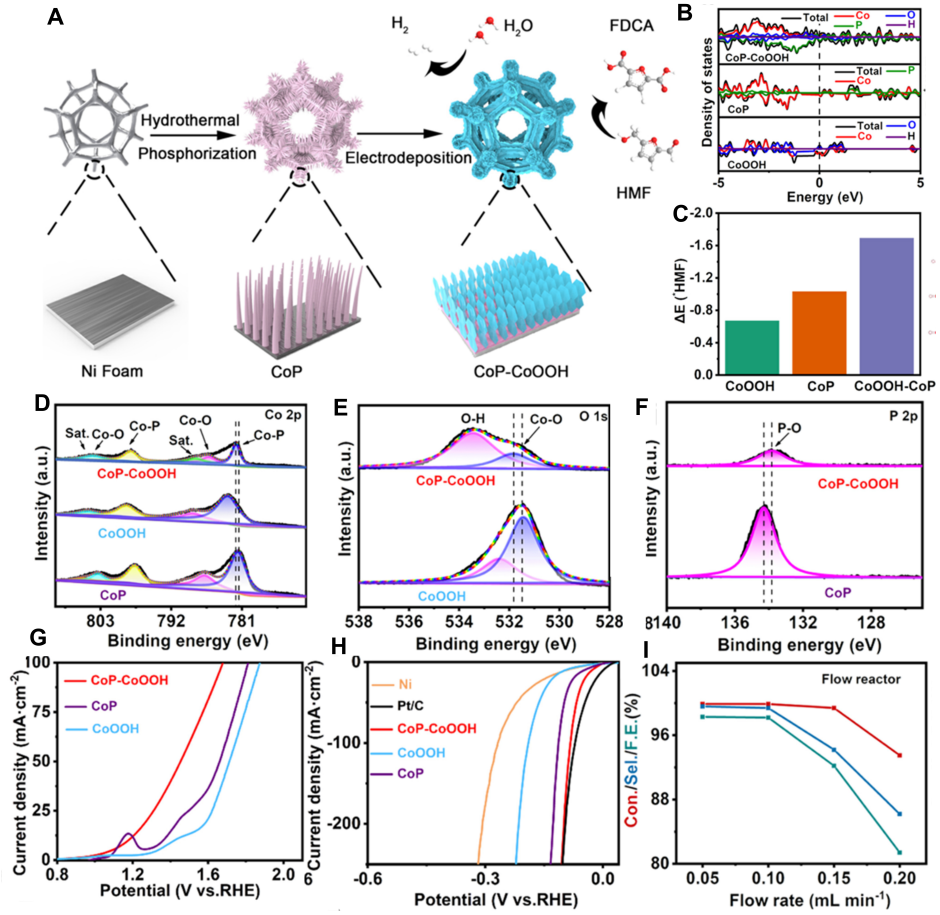

Figure 8. (A) Schematic illustration of the synthesis of the CoP-CoOOH. (B) Density of states and (C) HMF adsorption energy of CoP-CoOOH, CoP, and CoOOH. The XPS spectra of (D) Co 2p, (E) O 1s, and (F) P 2p. Polarization curves for (G) HMFOR and (H) hydrogen evolution. (I) HMF conversion, FDCA selectivity, and FE at flow reactor. Reproduced with permission[104]. Copyright 2022, Elsevier.

This unique structure creates a highly open channel for reactant transport and electrolyte permeation, which ultimately enhances catalytic performance. Kang *et al.* investigated the catalytic activity of Co_3O_4 and $NiCo_2O_4$ with a spinel structure for HMFOR[61]. The synthesized catalysts are all filamentous nanostructures composed of one-dimensional arranged nanoparticles [Figure 10C and D]. Among them, the $NiCo_2O_4$ filamentous structure demonstrates excellent HMF conversion rate (99.6%), successful recovery within three cycles of HMFOR, and over 80% FDCA conversion efficiency. Yan *et al.* synthesized a nano band array of vanadium oxide graded microspheres (VO_x-ms) [Figure 10E-J], which served as a catalyst for the selective oxidation of HMF to DFF with conversion and selectivity of 93.7% and 95.4%, respectively[109]. The exceptional performance is attributed to the exposure of the (010) surface, the vanadium-based (V=O) site with the highest hydrogen adsorption capacity, and the controlled highly oriented morphology that facilitates reactant contact.

Generally speaking, thinner sheets can expose more metal active sites. Zhang *et al.* synthesized ultra-thin NiCoFe-LDHs nanosheets (1.36 nm) using an improved co-precipitation method. Research has shown that introducing Fe into NiCo-LDHs can reduce the stacking effect of metal layers and reduce the thickness of nanosheets [Figure 10K-P][110]. The increased exposure of active sites promotes better contact between metals and oxygen or HMF, resulting in HMF oxidation occurring at lower potential regions.

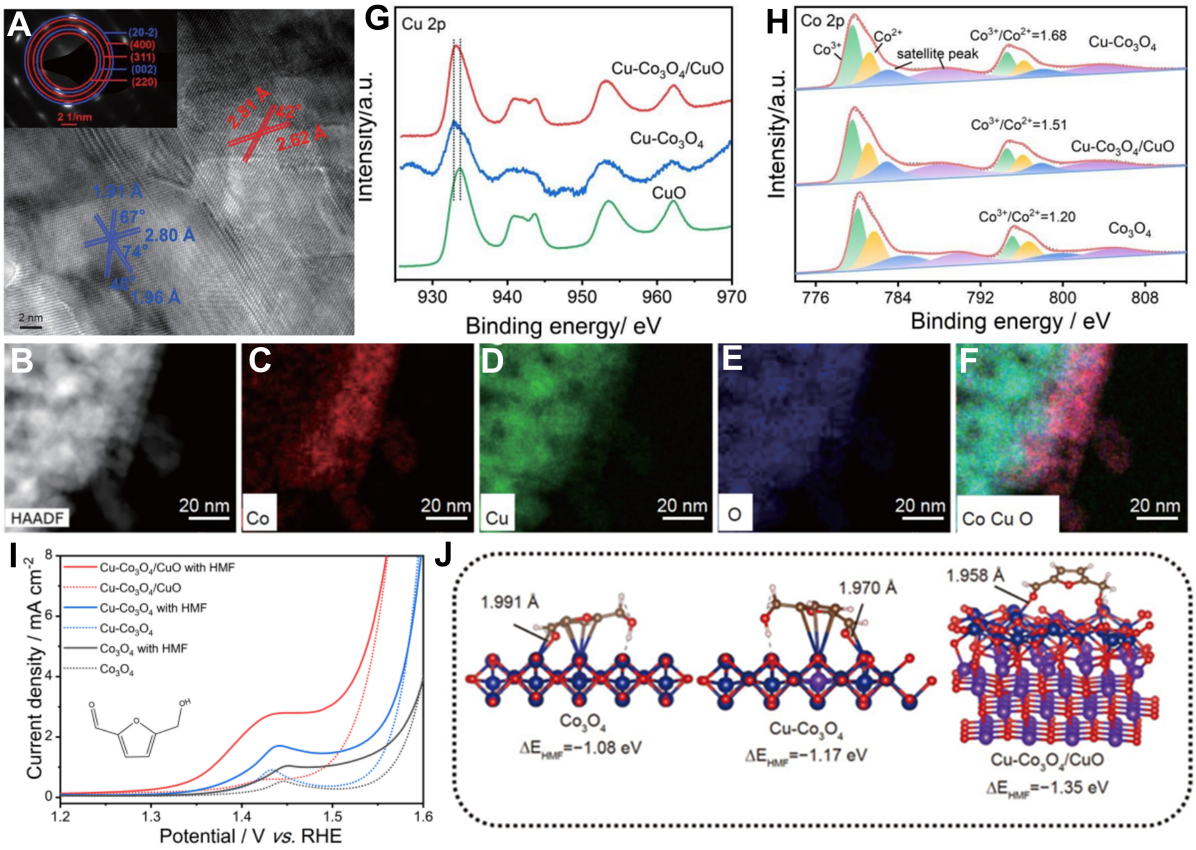

Figure 9. (A) HRTEM images of Cu-Co_3O_4/CuO. (B-F) high-angle annular dark field and element mapping images of Cu-Co_3O_4/CuO. (G) Cu 2p XPS spectra. (H) Co 2p XPS spectra. (I) The LSV curves in 1 M KOH with 10 mM HMF. (J) Relaxed adsorption structures of HMF on Co_3O_4, Cu-Co_3O_4, and Cu-Co_3O_4/CuO. Reproduced with permission[105]. Copyright 2023, Springer Nature.

Recently, there has been growing interest in core-shell structures due to their unique structural characteristics. This design is believed to effectively utilize the advantages of both the core and shell materials, optimize the geometric and electronic properties of the surface shell metal, and enable the shell to exhibit enhanced electrochemical activity and stability during interface reactions. Gao *et al.* discovered that the high HMF conversion energy of NiSe@NiO_x electrocatalysts is attributed to the distinct core-shell structure, which consists of a conductive NiSe framework and an active NiO_x surface layer[111]. Similarly, Deng *et al.* prepared Cu_xS@NiCo-LDHs nanosheet core-shell array serves as an efficient electrocatalyst for both HMF oxidation and H_2 release[112]. The metal properties of the Cu_xS core provide enough conductivity for the electrodeposition of active material NiCo-LDH, ensuring rapid charge transfer from the conductive substrate (Cu foam) to the catalytic layer on the shell surface. The combination of Co/Ni interactions in LDH shell with open nanostructures results in Cu_xS@NiCo-LDHs demonstrating excellent electrocatalytic activity and durability. The FE for both FDCA and H_2 production is close to one. As a bifunctional catalyst, H_2 and FDCA can be simultaneously produced at a current density of 10 mA cm^{-2} with a potential of only 1.34 V *vs.* RHE in a dual electrode electrolytic cell.

Multi-metal synergies

Due to enhanced conductivity or alternating chemical states of metal ions, the catalytic activity of multi-metal compounds is generally higher than that of single metal compounds[61,113-117]. Therefore, constructing synergistic multi-metal active sites to optimize the electronic structure of catalysts and thereby enhance the electrocatalytic performance for HMFOR is considered an effective strategy.

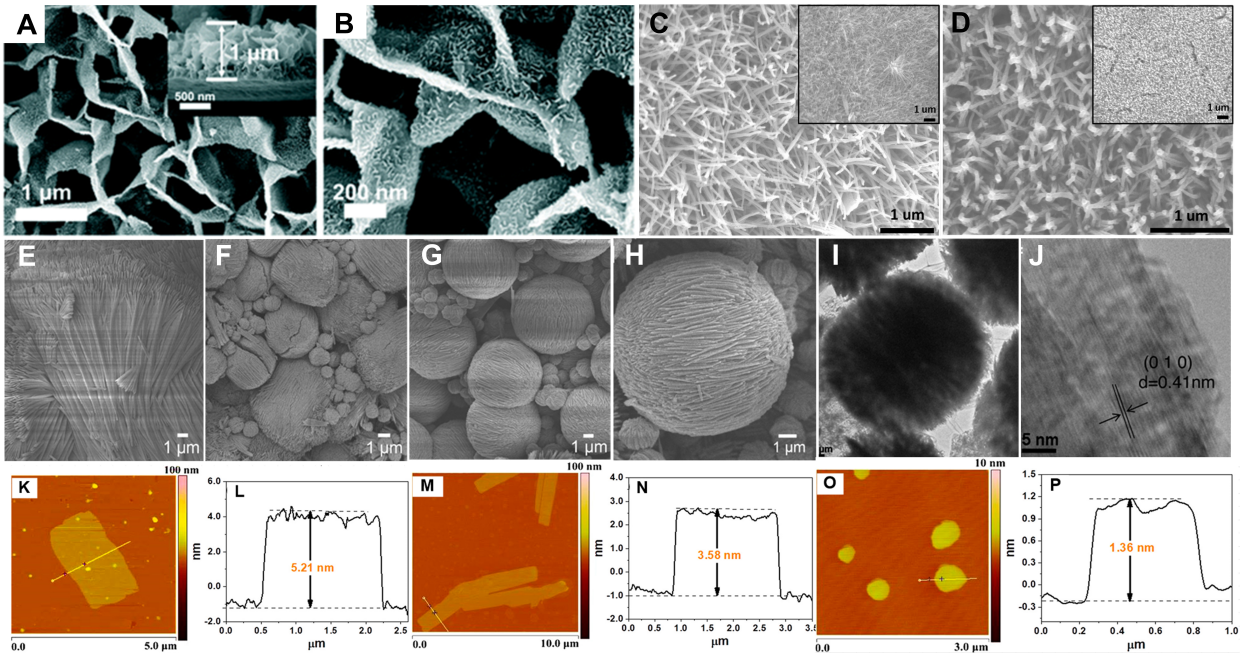

Figure 10. (A and B) SEM images of NiCo-S[108]. Copyright 2022, Royal Society of Chemistry. SEM images of (C) Co_3O_4 and (D) $NiCo_2O_4$[61]. Copyright 2019, Elsevier. FESEM images of VO_x-ms synthesized at 200 °C for (E) 15 min, (F) 30 min, (G) 1.5 h, (H) high magnification FESEM image of single VO_x-ms after calcination, (I) TEM image of VO_x-ms, (J) HRTEM of nanoparticles forming the nanobelts of VO_x-ms[109]. Copyright 2017, Elsevier. AFM images and height profiles of (K and L) NiCo-LDHs, (M and N) NiFe-LDHs, and (O and P) NiCoFe-LDHs. Reproduced with permission[110]. Copyright 2020, ACS Catalysis.

Zhao *et al.* reported the effects of bimetallic coordination and coordination effects on the electrooxidation of HMF on NiCo-S catalysts[108]. The electrochemical tests reveal that the Co-S catalyst exhibits a lower initial potential, and the Ni-S catalyst shows a higher current density. The bimetallic sulfide NiCo-S demonstrates superior performance, with a higher current density of 23 mA cm^{-2} at 1.45 V *vs.* RHE, a lower initial potential of approximately 1.20 V *vs.* RHE, and a faster reaction rate [Figure 11A and B]. The analysis of products at different potentials demonstrates that Co-S displays significant selectivity towards HMFCA, regardless of the potential, while Ni-S exhibits high selectivity towards FDCA at high potentials (1.45 V *vs.* RHE) and no product formation at low potentials (1.3 V *vs.* RHE) [Figure 11C and D]. Based on experimental and theoretical calculations, the authors propose that both Co and Ni act as bimetallic active sites, synergistically promoting the oxidation of HMF. The strong double atom (O and C atoms) adsorption of the metal active sites on the aldehyde group and the S coordination facilitate the conversion of the aldehyde group to the carboxyl group, reducing the initial potential generated by HMFCA, while the latter further accelerates the reaction rate of FDCA generation. Additionally, the formation of bimetallic complexes alters the morphology and increases the number of exposed sites, leading to improved electrocatalytic performance.

Le *et al.* showcased the viability of utilizing amorphous cobalt cerium binary metal oxide $Co_8Ce_2O_x$ as an effective electrocatalyst for the selective conversion of HMF into valuable DFF products[118]. The presence of Ce element allows the electronic structure of the original metal oxide to be regulated; the positive shift of Co 2p and O 1s peaks indicates that electron transfer between Co and Ce through an O bridge [Figure 12A and B]. The Raman spectra shown in Figure 12C and D indicate that $Co_8Ce_2O_x$ exhibits a faster phase transition compared to CoO_x. Further analysis of the Raman spectra at 60 minutes using Lorentz

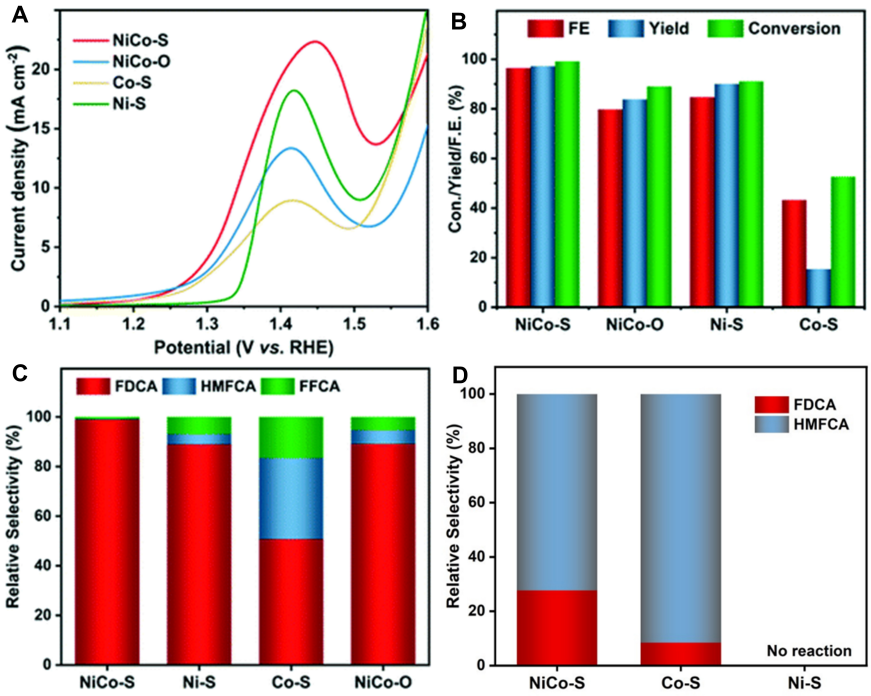

Figure 11. (A) The LSV of different catalysts. (B) Conversion of HMF and yield/FE/selectivity of FDCA (reaction time: 40 min). Relative selectivity of different products obtained by different electrodes at (C) 1.45 V *vs.* RHE and (D) 1.3 V *vs.* RHE. All the above tests were examined in 1 M KOH with 10 mM HMF. Reproduced with permission[108]. Copyright 2022, Royal Society of Chemistry.

fitting explains the transformation of the initial structure of the catalyst to the active phases of $CoOOH/CoO_2$ [Figure 12E and F]. The faster transformation rate of $Co_8Ce_2O_x$ accelerates the generation of a significant number of active species, thereby enhancing the kinetics of HMF oxidation.

Various binary LDHs are also regarded as promising electrocatalysts. In a study conducted by Liu *et al.*, NiFe-LDHs nanosheets were prepared on carbon fiber paper using a hydrothermal method[119]. These nanosheets prove to be efficient and durable catalysts for the direct electrochemical oxidation of HMF to FDCA. The addition of Fe increases the number of active sites and improves the catalytic activity of HMF electrochemical oxidation. In comparison to $Ni(OH)_2$ (1.28 V *vs.* RHE) nanosheets, NiFe-LDHs (1.25 V *vs.* RHE) exhibit a lower initial potential for HMF oxidation.

Furthermore, research has indicated that the integration of the three metal NiCoFe-LDHs brings together the advantages of both bimetallic NiCo- and NiFe-LDHs while also mitigating the drawbacks associated with the two parent materials. Zhang *et al.* prepared three metal NiCoFe-LDHs nanosheets by the method shown in Figure 13A and discovered that the inclusion of the third element Fe^{3+} alters the electronic environment of Ni^{2+} and Co^{2+}, and the peak position of the Ni 2p spectrum shifts towards a lower value, while the peak position of the Co 2p spectrum shifts towards a higher value [Figure 13B-D][110]. The presence of electronic synergies in NiCoFe-LDHs nanosheets enhances performance, as demonstrated by the lower overpotential (288 mV) for the OER reaction in comparison to bimetallic LDHs. Furthermore, the overpotential is further decreased with the addition of HMF [Figure 13E and F].

The above discussion has revealed that different modulation strategies can, to some extent, alter the geometric characteristics and electronic structure of catalysts, thereby optimizing intermediate adsorption,

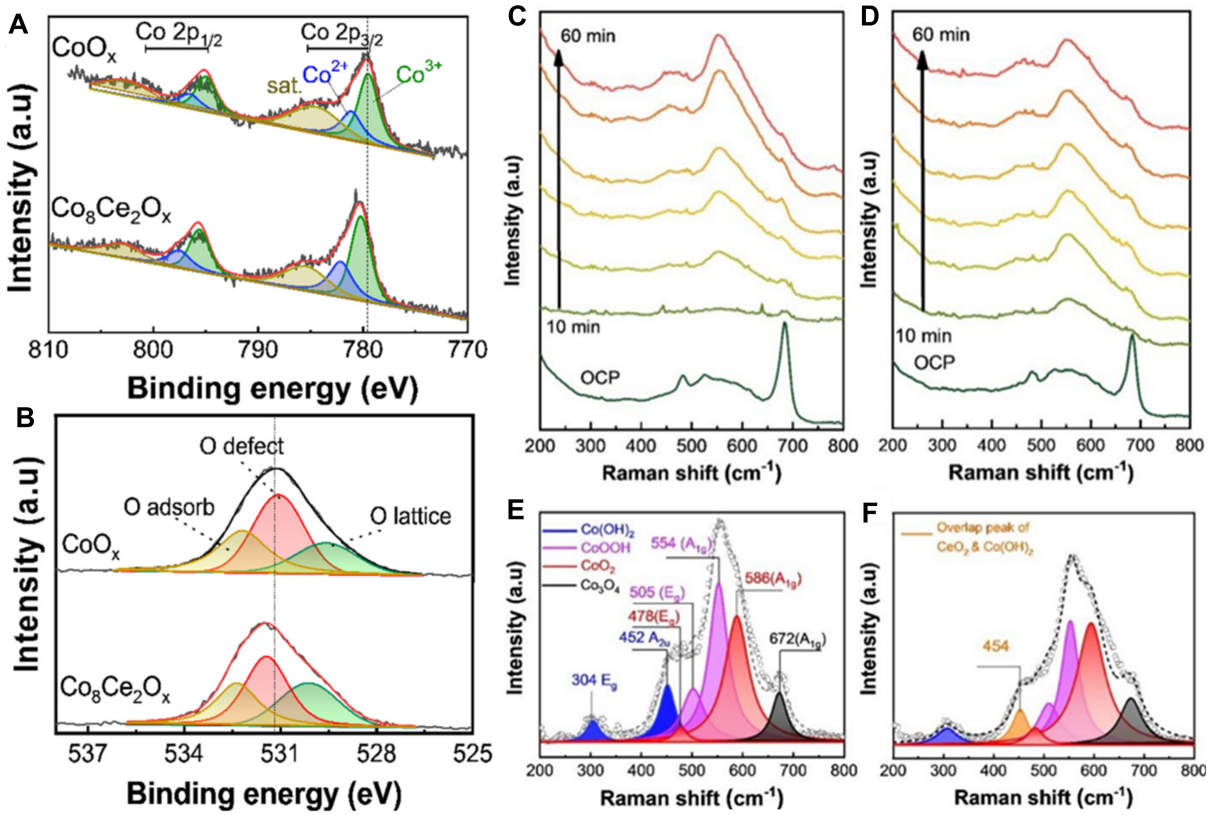

Figure 12. High-resolution XPS spectra of (A) Co 2p and (B) O 1s of $Co_8Ce_2O_x$. Operando Raman spectra of (C) CoO_x and (D) $Co_8Ce_2O_x$ under applied potential 1.60 V *vs.* RHE for HMF oxidation in pH = 13.0 electrolyte. The Lorentz peak function fit of (E) CoO_x and (F) $Co_8Ce_2O_x$ spectra at 60 min. Reproduced with permission[118]. Copyright 2021, Elsevier.

increasing active sites, and affecting the HMFOR performance[120,121]. In order to facilitate readers and beginners in this field to compare their results and draw conclusions about the activity of their materials, we summarize the performance data of typical catalysts mentioned above in Table 1.

CONCLUSIONS AND PROSPECT

The development of water splitting devices comprising anode HMF oxidation with cathode hydrogen production presents multiple benefits. This system can surpass the technical challenges associated with hydrogen production through water electrolysis, lower energy consumption, and avert the risk of H_2/O_2 gas mixture explosions. Furthermore, the exploration and development of high-value-added products derived from HMF, a compound widely produced through biomass conversion, holds immense economic potential and societal benefits [Figure 14]. Therefore, the preparation of reliable HMFOR electrocatalysts and the investigation of mechanistic issues in the catalytic process will bring breakthroughs to biomass processing and hydrogen production through water electrolysis. Various regulation strategies, such as heteroatom doping, defect project, interface engineering, structural design, and multi-metal synergies, are being explored to enhance the performance of HMFOR catalysts, aiming to optimize intermediate adsorption, increase surface area and active sites by regulating the electronic or geometric structure of the catalyst. While progress has been made in this area, there remain limitations that need to be addressed. Future research work needs to further study the improvement of the catalytic performance and FDCA selectivity of electrocatalysts from the following aspects to achieve large-scale applications.

Table 1. Electrocatalytic HMFOR activities of different catalysts

Catalyst	Electrolyte	Tafel (mV dec^{-1})	Oxidation voltage (V *vs.* RHE)	HMF conversion (%)	FDCA yield (%)	FE (%)	Reference
$Co_{0.4}NiS$@NF	1 M KOH + 50 mM HMF	94	1.45	~100	> 99	> 99	[70]
NiCoBDC NF	0.1 M KOH + 10 mM HMF	60.8	1.55	-	99	78.8	[78]
Ce-Co_2P@NC	1 M KOH + 10 mM HMF	163	1.43	99.5	-	98.5	[79]
Ni-Co_2P	1 M KOH + 10 mM HMF	-	1.29	-	> 99	> 97	[80]
CoO/$CoSe_2$	1 M KOH + 10 mM HMF	89.2	1.43	-	99	97.9	[50]
V_o-NiO	1 M KOH + 100 mM HMF	47.3	1.42	99.7	99.2	85.7	[90]
$NiVW_v$ LMH	1 M KOH + 10 mM HMF	12.8	1.43	~100	99.2	-	[91]
d-NiFe-LDH/CP	1 M KOH + 10 mM HMF	102.1	1.48	97.35	96.8	84.47	[92]
Ni_3N@C	1 M KOH + 10 mM HMF	48.9	1.45	-	98	99	[63]
Ni-MOF/Ag	1 M KOH + 10 mM HMF	-	1.62	~100	-	98.6	[96]
CoP-CoOOH	1 M KOH + 150 mM HMF	58	1.42	98.3	96.3	96.3	[104]
Cu-Co_3O_4/CuO	1 M KOH + 10 mM HMF	98.58	1.45	-	93	96	[105]
NiCo-S	1 M KOH + 10 mM HMF	-	1.45	99.1	97.1	96.4	[108]
$NiCo_2O_4$	1 M KOH + 5 mM HMF	135.7	1.5	90.4	90.8	87.5	[61]
NiSe@NiO_x	1 M KOH + 10 mM HMF	23	1.42	~100	99	99	[111]

Modulation strategies

The heteroatom doping strategy in HMFOR-HER systems primarily relies on cation doping, and there is a need for more research on the impact and mechanism of anion doping. Furthermore, multi-atom doping may offer more promising prospects compared to single-atom doping due to the synergistic effects between different elements, although there are limited reports on this. In terms of defect projection strategies, the focus has mainly been on studying oxygen vacancies in the HMFOR-HER system, but catalysts with other anion vacancies, such as sulfur vacancies, selenium vacancies, or multiple vacancies, may hold significant potential. Interface engineering strategies commonly concentrate on electron rearrangement at the interface, with little attention given to amorphous and crystalline heterostructures. For structural design strategies, accurately synthesizing specific structures and achieving large-scale production is a huge challenge. Lastly, further research is needed on the synergistic strategy of multiple metals, particularly in constructing multiple metal active sites and accurately analyzing the effects of different active sites.

Decomposing problems

The conversion pathway of HMF to FDCA is influenced by the pH of the electrolyte. At pH > 13, the aldehyde group undergoes oxidation to form HMFCA intermediates, with OH^- indirectly providing oxygen atoms. At pH < 13, the hydroxyl group is first oxidized to produce DFF intermediates. A higher pH leads to increased adsorption of hydroxyl groups on the catalyst surface, which enhances the activation of C-H/O-H bonds. In summary, OH^- plays a crucial role and accelerates the electrochemical oxidation reaction of HMF under high pH conditions. However, HMF tends to degrade into humic products in highly alkaline

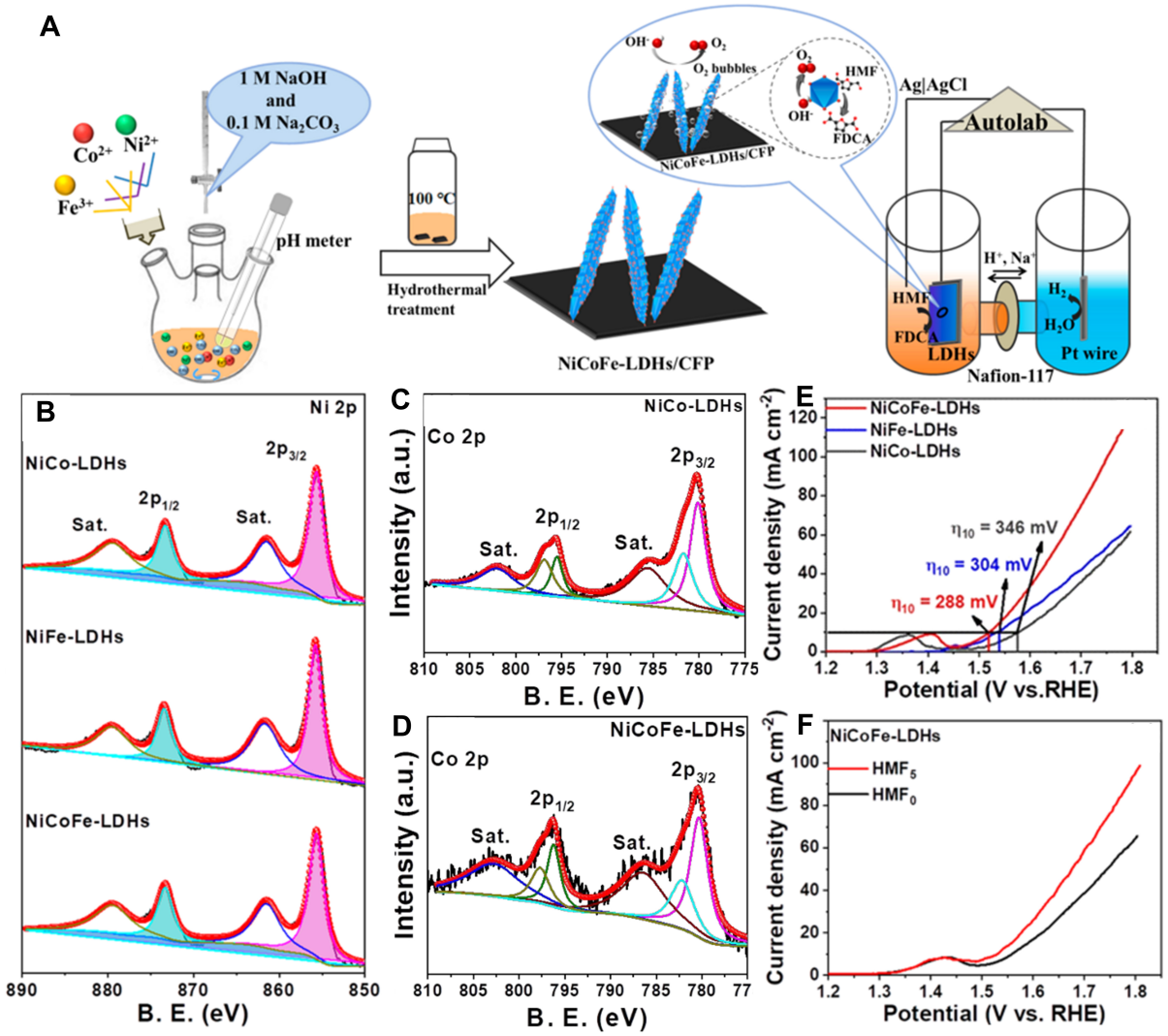

Figure 13. (A) Schematic illustration of NiCoFe-LDHs materials (left side) and the electrochemical system of HMFOR (right side). XPS spectra of (B) Ni 2p of the as-prepared NiCo-, NiFe-, and NiCoFe-LDHs. XPS spectra of Co 2p region of the as-prepared (C) NiCo-LDHs and (D) NiCoFe-LDHs. LSV curves of (E) OER and (F) HMFOR. Reproduced with permission[110]. Copyright 2020, ACS Catalysis.

solutions, which is detrimental to the reaction. How to balance the electrolytic conditions, HMF self-degradation and the electrolytic time remains a critical issue for future research.

Dual function issues

In general, acidic conditions are favorable for HER processes, while alkaline conditions are more conducive to HMFOR. However, the drawback of acidic conditions is their tendency to cause corrosion in equipment, which hinders large-scale industrial applications. Therefore, it is of great significance to reasonably design and develop catalysts with excellent HER and HMFOR performance in alkaline electrolytes and to try to reduce the overpotential of both reactions simultaneously. This places higher demands on material design. Future research should focus on integrating active components and constructing dual functional catalysts for HER and HMFOR to enhance the electrocatalytic performance of the overall system.

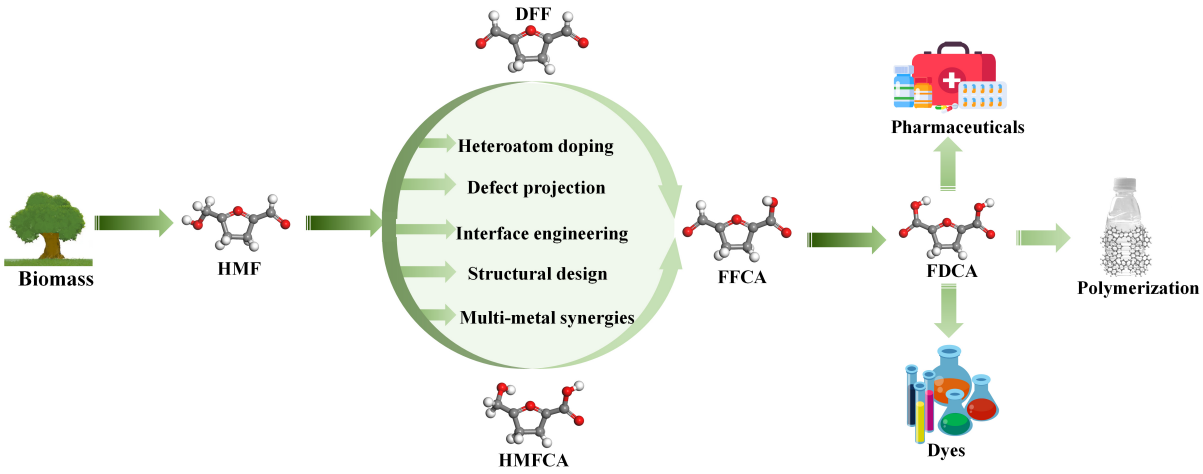

Figure 14. HMF conversion process and FDCA application foreground diagram.

Competition between OER and HMFOR

The utilization of HMFOR instead of OER leads to the inevitable occurrence of OER side reactions due to the overlapping potential range of the two reactions. Additionally, most catalysts that demonstrate remarkable performance for HMFOR in alkaline electrolytes also exhibit high activity for OER. This intrinsic excellent OER activity of the catalyst significantly restricts the activity and potential range of HMFOR, resulting in low FE. Consequently, it is imperative to conduct comprehensive research on the active components of catalysts for HMFOR and competitive OER. Exploring ways to enhance the kinetics of HMFOR, extending the Faradaic window for HMFOR, and minimizing the competitive OER process are crucial steps in this direction.

Stability issues

At present, the majority of catalysts that have been examined demonstrate the ability to sustain high levels of catalytic activity at low current densities. However, they fail to maintain stability over extended periods of time when subjected to demanding conditions, such as industrial-scale high current densities. Consequently, it is necessary to design catalysts reasonably and pay attention to stability while further improving catalytic activity, to achieve efficient hydrogen production and conversion of HMF under high current density conditions.

In-depth investigation into the reaction mechanism

Currently, the primary emphasis in HMF electrocatalysis research lies in the development and adjustment of catalysts. However, there is a limited focus on understanding the specific mechanism behind the electrocatalytic reaction of HMF. Developing additional characterization techniques to explore the mechanism of HMFOR is crucial. As mentioned above, research on the HMFOR mechanism is still in its early stages, requiring more precise evidence to explain the exact mechanism of HMFOR. Comprehensively understanding the mechanism is fundamental for guiding the development of next-generation HMFOR catalysts.

DECLARATIONS

Authors' contributions

Made substantial contributions to the conception and design of the study, performed data acquisition, and wrote the original draft: Zhang T, Liu S, Liu Q

Contributed to conceptualization, supervision, and writing - review & editing: Wang F, He X, Zhang X, Liu W, Liu X

Availability of data and materials
Not applicable.

Financial support and sponsorship
This work was financially supported by the National Natural Science Foundation of China (22075211 and 22275166), and Guangxi Natural Science Fund for Distinguished Young Scholars (2024GXNSFFA010008).

Conflicts of interest
All authors declared that there are no conflicts of interest.

Ethical approval and consent to participate
Not applicable.

Consent for publication
Not applicable.

REFERENCES
1. Kumar A, Daw P, Milstein D. Homogeneous catalysis for sustainable energy: hydrogen and methanol economies, fuels from biomass, and related topics. *Chem Rev* 2022;122:385-441. DOI PubMed PMC
2. Ganguly S, Paul S, Khurana D, et al. Ternary Ni-Co-Se nanostructure for electrocatalytic oxidative value addition of biomass platform chemicals. *ACS Appl Energy Mater* 2023;6:5331-41. DOI
3. Chu S, Majumdar A. Opportunities and challenges for a sustainable energy future. *Nature* 2012;488:294-303. DOI PubMed
4. Chu S, Cui Y, Liu N. The path towards sustainable energy. *Nat Mater* 2016;16:16-22. DOI PubMed
5. Morais AR, da Costa Lopes AM, Bogel-Łukasik R. Carbon dioxide in biomass processing: contributions to the green biorefinery concept. *Chem Rev* 2015;115:3-27. DOI
6. Climent MJ, Corma A, Iborra S. Converting carbohydrates to bulk chemicals and fine chemicals over heterogeneous catalysts. *Green Chem* 2011;13:520. DOI
7. Huang CJ, Xu HM, Shuai TY, Zhan QN, Zhang ZJ, Li GR. Modulation strategies for the preparation of high-performance catalysts for urea oxidation reaction and their applications. *Small* 2023;19:e2301130. DOI PubMed
8. Zhao G, Rui K, Dou SX, Sun W. Heterostructures for electrochemical hydrogen evolution reaction: a review. *Adv Funct Mater* 2018;28:1803291. DOI
9. Wei J, Zhou M, Long A, et al. Heterostructured electrocatalysts for hydrogen evolution reaction under alkaline conditions. *Nanomicro Lett* 2018;10:75. DOI PubMed PMC
10. Yu W, Gao Y, Chen Z, Zhao Y, Wu Z, Wang L. Strategies on improving the electrocatalytic hydrogen evolution performances of metal phosphides. *Chin J Catal* 2021;42:1876-902. DOI
11. Zhu B, Liang Z, Zou R. Designing advanced catalysts for energy conversion based on urea oxidation reaction. *Small* 2020;16:e1906133. DOI PubMed
12. Jacobson MZ. Review of solutions to global warming, air pollution, and energy security. *Energy Environ Sci* 2009;2:148-73. DOI
13. Yu ZY, Duan Y, Feng XY, Yu X, Gao MR, Yu SH. Clean and affordable hydrogen fuel from alkaline water splitting: past, recent progress, and future prospects. *Adv Mater* 2021;33:e2007100. DOI PubMed
14. Qin Y, Cao H, Liu Q, et al. Multi-functional layered double hydroxides supported by nanoporous gold toward overall hydrazine splitting. *Front Chem Sci Eng* 2024;18:6. DOI
15. Liu W, Que W, Yin R, et al. Ferrum-molybdenum dual incorporated cobalt oxides as efficient bifunctional anti-corrosion electrocatalyst for seawater splitting. *Appl Catal B Environ* 2023;328:122488. DOI
16. Li W, Liu K, Feng S, et al. Well-defined Ni_3N nanoparticles armored in hollow carbon nanotube shell for high-efficiency bifunctional hydrogen electrocatalysis. *J Colloid Interface Sci* 2024;655:726-35. DOI
17. Ding J, Yang H, Zhang H, et al. Dealloyed NiTiZrAg as an efficient electrocatalyst for hydrogen evolution in alkaline seawater. *Int J Hydrog Energy* 2023;53:318-24. DOI

18. Liu W, Niu X, Tang J, et al. Energy-efficient anodic reactions for sustainable hydrogen production via water electrolysis. *Chem Synth* 2023;3:44. DOI
19. Guo L, Wang J, Teng X, Liu Y, He X, Chen Z. A novel bimetallic nickel-molybdenum carbide nanowire array for efficient hydrogen evolution. *ChemSusChem* 2018;11:2717-23. DOI
20. Mahmood N, Yao Y, Zhang JW, Pan L, Zhang X, Zou JJ. Electrocatalysts for hydrogen evolution in alkaline electrolytes: mechanisms, challenges, and prospective solutions. *Adv Sci* 2018;5:1700464. DOI PubMed PMC
21. Ji Y, Yu Z, Yan L, Song W. Research progress in preparation, modification and application of biomass-based single-atom catalysts. *China Powder Sci Technol* 2023;29:100-7. DOI
22. Nicita A, Maggio G, Andaloro A, Squadrito G. Green hydrogen as feedstock: financial analysis of a photovoltaic-powered electrolysis plant. *Int J Hydrogen Energ* 2020;45:11395-408. DOI
23. Zou X, Zhang Y. Noble metal-free hydrogen evolution catalysts for water splitting. *Chem Soc Rev* 2015;44:5148-80. DOI PubMed
24. Lagadec MF, Grimaud A. Water electrolysers with closed and open electrochemical systems. *Nat Mater* 2020;19:1140-50. DOI PubMed
25. Liu X, Guo R, Ni K, et al. Reconstruction-determined alkaline water electrolysis at industrial temperatures. *Adv Mater* 2020;32:e2001136. DOI
26. Wang C, Lu H, Mao Z, Yan C, Shen G, Wang X. Bimetal schottky heterojunction boosting energy-saving hydrogen production from alkaline water via urea electrocatalysis. *Adv Funct Mater* 2020;30:2000556. DOI
27. Zhou L, Shao M, Zhang C, et al. Hierarchical CoNi-sulfide nanosheet arrays derived from layered double hydroxides toward efficient hydrazine electrooxidation. *Adv Mater* 2017;29:1604080. DOI
28. Tao HB, Xu Y, Huang X, et al. A General method to probe oxygen evolution intermediates at operating conditions. *Joule* 2019;3:1498-509. DOI
29. Huang H, Yu C, Han X, et al. Ni, Co hydroxide triggers electrocatalytic production of high-purity benzoic acid over 400 mA cm^{-2}. *Energy Environ Sci* 2020;13:4990-9. DOI
30. Lie WH, Yang Y, Yuwono JA, et al. Identification of catalytic activity descriptors for selective 5-hydroxymethyl furfural electrooxidation to 2,5-furandicarboxylic acid. *J Mater Chem A* 2023;11:5527-39. DOI
31. Mondal B, Karjule N, Singh C, et al. Unraveling the mechanisms of electrocatalytic oxygenation and dehydrogenation of organic molecules to value-added chemicals over a Ni-Fe oxide catalyst. *Adv Energy Mater* 2021;11:2101858. DOI
32. Chen Y, Tian B, Cheng Z, et al. Electro-descriptors for the performance prediction of electro-organic synthesis. *Angew Chem Int Ed* 2021;60:4199-207. DOI
33. Danish M, Ahmad T. A review on utilization of wood biomass as a sustainable precursor for activated carbon production and application. *Renew Sust Energ Rev* 2018;87:1-21. DOI
34. Sudarsanam P, Zhong R, Van den Bosch S, Coman SM, Parvulescu VI, Sels BF. Functionalised heterogeneous catalysts for sustainable biomass valorisation. *Chem Soc Rev* 2018;47:8349-402. DOI PubMed
35. Venkata Mohan S, Nikhil GN, Chiranjeevi P, et al. Waste biorefinery models towards sustainable circular bioeconomy: critical review and future perspectives. *Bioresour Technol* 2016;215:2-12. DOI
36. Xu C, Paone E, Rodríguez-Padrón D, Luque R, Mauriello F. Recent catalytic routes for the preparation and the upgrading of biomass derived furfural and 5-hydroxymethylfurfural. *Chem Soc Rev* 2020;49:4273-306. DOI PubMed
37. Verdeguer P, Merat N, Gaset A. Oxydation catalytique du HMF en acide 2,5-furane dicarboxylique. *J Mol Catal* 1993;85:327-44. DOI
38. Hu L, He A, Liu X, et al. Biocatalytic Transformation of 5-hydroxymethylfurfural into high-value derivatives: recent advances and future aspects. *ACS Sustain Chem Eng* 2018;6:15915-35. DOI
39. Tong X, Ma Y, Li Y. Biomass into chemicals: conversion of sugars to furan derivatives by catalytic processes. *Appl Catal A Gen* 2010;385:1-13. DOI
40. Payne KAP, Marshall SA, Fisher K, et al. Enzymatic carboxylation of 2-furoic acid yields 2,5-furandicarboxylic acid (FDCA). *ACS Catal* 2019;9:2854-65. DOI PubMed PMC
41. Eerhart AJJE, Faaij APC, Patel MK. Replacing fossil based PET with biobased PEF; process analysis, energy and GHG balance. *Energy Environ Sci* 2012;5:6407. DOI
42. Zhang H, Qi G, Liu W, et al. Bimetallic phosphoselenide nanosheets as bifunctional catalysts for 5-hydroxymethylfurfural oxidation and hydrogen evolution. *Inorg Chem Front* 2023;10:2423-9. DOI
43. Xu Y, Jia X, Ma J, et al. Efficient synthesis of 2,5-dicyanofuran from biomass-derived 2,5-diformylfuran via an oximation-dehydration strategy. *ACS Sustain Chem Eng* 2018;6:2888-92. DOI
44. Zhang C, Xu H, Wang Y, et al. Reduction of 4-nitrophenol with nano-gold@graphene composite porous material. *China Powder Sci Technol* 2023;29:80-93. DOI
45. Yang Y, Mu T. Electrochemical oxidation of biomass derived 5-hydroxymethylfurfural (HMF): pathway, mechanism, catalysts and coupling reactions. *Green Chem* 2021;23:4228-54. DOI
46. Ma C, Fang P, Mei T. Recent advances in C-H functionalization using electrochemical transition metal catalysis. *ACS Catal* 2018;8:7179-89. DOI
47. Giannakoudakis DA, Colmenares JC, Tsiplakides D, Triantafyllidis KS. Nanoengineered electrodes for biomass-derived 5-hydroxymethylfurfural electrocatalytic oxidation to 2,5-furandicarboxylic acid. *ACS Sustain Chem Eng* 2021;9:1970-93. DOI

48. Zhou H, Li Z, Ma L, Duan H. Electrocatalytic oxidative upgrading of biomass platform chemicals: from the aspect of reaction mechanism. *Chem Commun* 2022;58:897-907. DOI
49. Yang M, Meng G, Li H, et al. Bifunctional bimetallic oxide nanowires for high-efficiency electrosynthesis of 2,5-furandicarboxylic acid and ammonia. *J Colloid Interface Sci* 2023;652:155-63. DOI
50. Huang X, Song J, Hua M, et al. Enhancing the electrocatalytic activity of CoO for the oxidation of 5-hydroxymethylfurfural by introducing oxygen vacancies. *Green Chem* 2020;22:843-9. DOI
51. Wei T, Liu W, Zhang S, Liu Q, Luo J, Liu X. A dual-functional Bi-doped Co_3O_4 nanosheet array towards high efficiency 5-hydroxymethylfurfural oxidation and hydrogen production. *Chem Commun* 2023;59:442-5. DOI
52. Grabowski G, Lewkowski J, Skowroński R. The electrochemical oxidation of 5-hydroxymethylfurfural with the nickel oxide/hydroxide electrode. *Electrochim Acta* 1991;36:1995. DOI
53. Liu W, Cui Y, Du X, Zhang Z, Chao Z, Deng Y. High efficiency hydrogen evolution from native biomass electrolysis. *Energy Environ Sci* 2016;9:467-72. DOI
54. Zhang B, Fu H, Mu T. Hierarchical NiS_x/Ni_2P nanotube arrays with abundant interfaces for efficient electrocatalytic oxidation of 5-hydroxymethylfurfural. *Green Chem* 2022;24:877-84. DOI
55. Yang G, Jiao Y, Yan H, et al. Interfacial engineering of MoO_2-FeP heterojunction for highly efficient hydrogen evolution coupled with biomass electrooxidation. *Adv Mater* 2020;32:e2000455. DOI
56. Wang D, Chen C, Wang S. Defect engineering for advanced electrocatalytic conversion of nitrogen-containing molecules. *Sci China Chem* 2023;66:1052-72. DOI
57. Vuyyuru KR, Strasser P. Oxidation of biomass derived 5-hydroxymethylfurfural using heterogeneous and electrochemical catalysis. *Catal Today* 2012;195:144-54. DOI
58. Cha HG, Choi KS. Combined biomass valorization and hydrogen production in a photoelectrochemical cell. *Nat Chem* 2015;7:328-33. DOI
59. Lu Y, Dong CL, Huang YC, et al. Identifying the geometric site dependence of spinel oxides for the electrooxidation of 5-hydroxymethylfurfural. *Angew Chem Int Ed* 2020;59:19215-21. DOI
60. Lu Y, Liu T, Dong CL, et al. Tuning the selective adsorption site of biomass on Co_3O_4 by Ir single atoms for electrosynthesis. *Adv Mater* 2021;33:e2007056. DOI
61. Kang MJ, Park H, Jegal J, Hwang SY, Kang YS, Cha HG. Electrocatalysis of 5-hydroxymethylfurfural at cobalt based spinel catalysts with filamentous nanoarchitecture in alkaline media. *Appl Catal B Environ* 2019;242:85-91. DOI
62. Lu Y, Dong C, Huang Y, et al. Hierarchically nanostructured NiO-Co_3O_4 with rich interface defects for the electro-oxidation of 5-hydroxymethylfurfural. *Sci China Chem* 2020;63:980-6. DOI
63. Zhang N, Zou Y, Tao L, et al. Electrochemical oxidation of 5-hydroxymethylfurfural on nickel nitride/carbon nanosheets: reaction pathway determined by in situ sum frequency generation vibrational spectroscopy. *Angew Chem Int Ed* 2019;58:15895-903. DOI
64. Wang H, Li C, An J, Zhuang Y, Tao S. Surface reconstruction of NiCoP for enhanced biomass upgrading. *J Mater Chem A* 2021;9:18421-30. DOI
65. Barwe S, Weidner J, Cychy S, et al. Electrocatalytic Oxidation of 5-(Hydroxymethyl)furfural using high-surface-area nickel boride. *Angew Chem Int Ed* 2018;57:11460-4. DOI
66. You B, Jiang N, Liu X, Sun Y. Simultaneous H_2 generation and biomass upgrading in water by an efficient noble-metal-free bifunctional electrocatalyst. *Angew Chem Int Ed* 2016;55:9913-7. DOI PubMed
67. Holzhäuser FJ, Janke T, Öztas F, Broicher C, Palkovits R. Electrocatalytic oxidation of 5-hydroxymethylfurfural into the monomer 2,5-furandicarboxylic acid using mesostructured nickel oxide. *Adv Sustain Syst* 2020;4:1900151. DOI
68. Guo M, Lu X, Xiong J, Zhang R, Li X, et al. Alloy-driven efficient electrocatalytic oxidation of biomass-derived 5-hydroxymethylfurfural towards 2,5-furandicarboxylic acid: a review. *ChemSusChem* 2022;17:e202201074. DOI
69. Zhao Y, Cai M, Xian J, Sun Y, Li G. Recent advances in the electrocatalytic synthesis of 2,5-furandicarboxylic acid from 5-(hydroxymethyl)furfural. *J Mater Chem A* 2021;9:20164-83. DOI
70. Sun Y, Wang J, Qi Y, Li W, Wang C. Efficient electrooxidation of 5-hydroxymethylfurfural using Co-doped Ni_3S_2 catalyst: promising for H_2 production under industrial-level current density. *Adv Sci* 2022;9:e2200957. DOI PubMed PMC
71. An L, Zhao X, Zhao T, Wang D. Atomic-level insight into reasonable design of metal-based catalysts for hydrogen oxidation in alkaline electrolytes. *Energy Environ Sci* 2021;14:2620-38. DOI
72. Li F, Bu Y, Lv Z, et al. Porous cobalt phosphide polyhedrons with iron doping as an efficient bifunctional electrocatalyst. *Small* 2017;13:40. DOI
73. Zhao Y, Dongfang N, Triana CA, et al. Dynamics and control of active sites in hierarchically nanostructured cobalt phosphide/chalcogenide-based electrocatalysts for water splitting. *Energy Environ Sci* 2022;15:727-39. DOI PubMed PMC
74. Chen D, Chen Z, Zhang X, et al. Exploring single atom catalysts of transition-metal doped phosphorus carbide monolayer for HER: a first-principles study. *J Energy Chem* 2021;52:155-62. DOI
75. Fei B, Chen Z, Liu J, et al. Ultrathinning nickel sulfide with modulated electron density for efficient water splitting. *Adv Energy Mater* 2020;10:2001963. DOI
76. Jin C, Zhai P, Wei Y, et al. $Ni(OH)_2$ templated synthesis of ultrathin Ni_3S_2 nanosheets as bifunctional electrocatalyst for overall water splitting. *Small* 2021;17:e2102097. DOI
77. Zhang L, Gao X, Zhu Y, et al. Electrocatalytically inactive copper improves the water adsorption/dissociation on Ni_3S_2 for

accelerated alkaline and neutral hydrogen evolution. *Nanoscale* 2021;13:2456-64. DOI

78. Cai M, Zhang Y, Zhao Y, Liu Q, Li Y, Li G. Two-dimensional metal-organic framework nanosheets for highly efficient electrocatalytic biomass 5-(hydroxymethyl)furfural (HMF) valorization. *J Mater Chem A* 2020;8:20386-92. DOI
79. Xie S, Fu H, Chen L, Li Y, Shen K. Carbon-based nanoarrays embedded with Ce-doped ultrasmall Co2P nanoparticles enable efficient electrooxidation of 5-hydroxymethylfurfural coupled with hydrogen production. *Sci China Chem* 2023;66:2141-52. DOI
80. Li J, Mao X, Gong W, et al. Engineering active Ni-doped Co_2P catalyst for efficient electrooxidation coupled with hydrogen evolution. *Nano Res* 2023;16:6728-35. DOI
81. Gao P, Chen Z, Gong Y, et al. The role of cation vacancies in electrode materials for enhanced electrochemical energy storage: synthesis, advanced characterization, and fundamentals. *Adv Energy Mater* 2020;10:1903780. DOI
82. Liu X, Zhang L, Zheng Y, et al. Uncovering the effect of lattice strain and oxygen deficiency on electrocatalytic activity of perovskite cobaltite thin films. *Adv Sci* 2019;6:1801898. DOI PubMed PMC
83. Liu G, Li J, Fu J, et al. An oxygen-vacancy-rich semiconductor-supported bifunctional catalyst for efficient and stable zinc-air batteries. *Adv Mater* 2019;31:e1806761. DOI
84. Asnavandi M, Yin Y, Li Y, Sun C, Zhao C. Promoting oxygen evolution reactions through introduction of oxygen vacancies to benchmark NiFe-OOH catalysts. *ACS Energy Lett* 2018;3:1515-20. DOI
85. Sun J, Guo N, Shao Z, et al. A facile strategy to construct amorphous spinel-based electrocatalysts with massive oxygen vacancies using ionic liquid dopant. *Adv Energy Mater* 2018;8:1800980. DOI
86. Ma L, Chen S, Pei Z, et al. Flexible waterproof rechargeable hybrid zinc batteries initiated by multifunctional oxygen vacancies-rich cobalt oxide. *ACS Nano* 2018;12:8597-605. DOI
87. Zhou D, Xiong X, Cai Z, et al. Flame-engraved nickel-iron layered double hydroxide nanosheets for boosting oxygen evolution reactivity. *Small Methods* 2018;2:1800083. DOI
88. Lu Y, Li C, Zhang Y, et al. Engineering of cation and anion vacancies in Co_3O_4 thin nanosheets by laser irradiation for more advancement of oxygen evolution reaction. *Nano Energy* 2021;83:105800. DOI
89. He J, Zhou X, Xu P, Sun J. Promoting electrocatalytic water oxidation through tungsten-modulated oxygen vacancies on hierarchical FeNi-layered double hydroxide. *Nano Energy* 2021;80:105540. DOI
90. Wang H, Zhang J, Tao S. Nickel oxide nanoparticles with oxygen vacancies for boosting biomass-upgrading. *Chem Eng J* 2022;444:136693. DOI
91. Zhang B, Yang Z, Yan C, Xue Z, Mu T. Operando forming of lattice vacancy defect in ultrathin crumpled NiVW-layered metal hydroxides nanosheets for valorization of biomass. *Small* 2023;19:e2207236. DOI
92. Qi Y, Wang K, Sun Y, Wang J, Wang C. Engineering the electronic structure of NiFe layered double hydroxide nanosheet array by implanting cationic vacancies for efficient electrochemical conversion of 5-hydroxymethylfurfural to 2,5-furandicarboxylic acid. *ACS Sustain Chem Eng* 2022;10:645-54. DOI
93. Tao L, Wang Y, Zou Y, et al. Charge transfer modulated activity of carbon-based electrocatalysts. *Adv Energy Mater* 2020;10:1901227. DOI
94. Zhang J, Zhang Q, Feng X. Support and interface effects in water-splitting electrocatalysts. *Adv Mater* 2019;31:e1808167. DOI
95. Sun X, Yuan K, Zhou J, Yuan C, Liu H, Zhang Y. Au^{3+} species-induced interfacial activation enhances metal-support interactions for boosting electrocatalytic CO_2 reduction to CO. *ACS Catal* 2022;12:923-34. DOI
96. Pang X, Zhao H, Huang Y, Luo B, Bai H, Fan W. Electrochemically induced NiOOH/Ag^+ active species for efficient oxidation of 5-hydroxymethylfurfural. *Appl Surf Sci* 2023;608:155152. DOI
97. Cheng Z, Xiao Y, Wu W, et al. All-pH-tolerant in-plane heterostructures for efficient hydrogen evolution reaction. *ACS Nano* 2021;15:11417-27. DOI
98. Yan C, Huang J, Sun K, et al. Cu_2ZnSnS_4 solar cells with over 10% power conversion efficiency enabled by heterojunction heat treatment. *Nat Energy* 2018;3:764-72. DOI
99. Jiang W, Zong X, An L, et al. Consciously constructing heterojunction or direct z-scheme photocatalysts by regulating electron flow direction. *ACS Catal* 2018;8:2209-17. DOI
100. Ma J, Su J, Lin Z, et al. Improve the oxide/perovskite heterojunction contact for low temperature high efficiency and stable all-inorganic $CsPbI_2Br$ perovskite solar cells. *Nano Energy* 2020;67:104241. DOI
101. Wang F, Yang H, Zhang H, et al. One-pot synthesis enables magnetic coupled Cr_2Te_3/MnTe/Cr_2Te_3 integrated heterojunction nanorods. *Nano Lett* 2021;21:7684-90. DOI
102. Chen S, Qi G, Yin R, et al. Electrocatalytic nitrate-to-ammonia conversion on CoO/CuO nanoarrays using Zn-nitrate batteries. *Nanoscale* 2023;15:19577-85. DOI
103. Xie Y, Sun L, Pan X, Zhou Z, Zhao G. Selective two-electron electrocatalytic conversion of 5-Hydroxymethylfurfural boosting hydrogen production under neutral condition over $Co(OH)_2$-CeO_2 catalyst. *Appl Catal B Environ* 2023;338:123068. DOI
104. Wang H, Zhou Y, Tao S. CoP-CoOOH heterojunction with modulating interfacial electronic structure: a robust biomass-upgrading electrocatalyst. *Appl Catal B Environ* 2022;315:121588. DOI
105. Guo J, Wang G, Cui S, et al. Enhanced adsorption with hydroxymethyl and aldehyde over the heterophase interface for efficient biomass electrooxidation. *Sci China Mater* 2023;66:2698-707. DOI
106. Qin Y, Han X, Li Y, et al. Hollow mesoporous metal-organic frameworks with enhanced diffusion for highly efficient catalysis. *ACS Catal* 2020;10:5973-8. DOI

107. Qin Y, Wang B, Qiu Y, et al. Multi-shelled hollow layered double hydroxides with enhanced performance for the oxygen evolution reaction. *Chem Commun* 2021;57:2752-5. DOI
108. Zhao Z, Guo T, Luo X, et al. Bimetallic sites and coordination effects: electronic structure engineering of NiCo-based sulfide for 5-hydroxymethylfurfural electrooxidation. *Catal Sci Technol* 2022;12:3817-25. DOI
109. Yan Y, Li K, Zhao J, Cai W, Yang Y, Lee J. Nanobelt-arrayed vanadium oxide hierarchical microspheres as catalysts for selective oxidation of 5-hydroxymethylfurfural toward 2,5-diformylfuran. *Appl Catal B Environ* 2017;207:358-65. DOI
110. Zhang M, Liu Y, Liu B, Chen Z, Xu H, Yan K. Trimetallic NiCoFe-layered double hydroxides nanosheets efficient for oxygen evolution and highly selective oxidation of biomass-derived 5-hydroxymethylfurfural. *ACS Catal* 2020;10:5179-89. DOI
111. Gao L, Liu Z, Ma J, et al. NiSe@NiOx core-shell nanowires as a non-precious electrocatalyst for upgrading 5-hydroxymethylfurfural into 2,5-furandicarboxylic acid. *Appl Catal B Environ* 2020;261:118235. DOI
112. Deng X, Kang X, Li M, et al. Coupling efficient biomass upgrading with H_2 production *via* bifunctional Cu_xS@NiCo-LDH core-shell nanoarray electrocatalysts. *J Mater Chem A* 2020;8:1138-46. DOI
113. Jadhav HS, Roy A, Chung W, Seo JG. Free standing growth of $MnCo_2O_4$ nanoflakes as an electrocatalyst for methanol electro-oxidation. *New J Chem* 2017;41:15058-63. DOI
114. Gao L, Bao Y, Gan S, et al. Hierarchical nickel-cobalt-based transition metal oxide catalysts for the electrochemical conversion of biomass into valuable chemicals. *ChemSusChem* 2018;11:2547-53. DOI
115. Yuan C, Hui KS, Yin H, et al. Regulating intrinsic electronic structures of transition-metal-based catalysts and the potential applications for electrocatalytic water splitting. *ACS Materials Lett* 2021;3:752-80. DOI
116. Feng J, Zheng D, Yin R, et al. A wide-temperature adaptive aqueous zinc-air battery-based on Cu-Co dual metal-nitrogen-carbon/nanoparticle electrocatalysts. *Small Struct* 2023;4:2200340. DOI
117. Zhang G, Wang G, Wan Y, Liu X, Chu K. Ampere-level nitrate electroreduction to ammonia over monodispersed Bi-Doped FeS_2. *ACS Nano* 2023;17:21328-36. DOI PubMed
118. Le T, Vo T, Chiang C. Highly efficient amorphous binary cobalt-cerium metal oxides for selective oxidation of 5-hydroxymethylfurfural to 2,5-diformylfuran. *J Catal* 2021;404:560-9. DOI
119. Liu W, Dang L, Xu Z, Yu H, Jin S, Huber GW. Electrochemical Oxidation of 5-hydroxymethylfurfural with NiFe layered double hydroxide (LDH) nanosheet catalysts. *ACS Catal* 2018;8:5533-41. DOI
120. Yang M, Wei T, He J, et al. Au nanoclusters anchored on TiO_2 nanosheets for high-efficiency electroreduction of nitrate to ammonia. *Nano Res* 2024;17:1209-16. DOI
121. Lu Z, Yang H, Liu Q, et al. Nb_2 AlC MAX nanosheets supported Ru nanocrystals as efficient catalysts for boosting pH-universal hydrogen production. *Small* 2023:e2305434. DOI